Studies on spectrophotometric analyses for ultratrace amounts of metal ions coupled with catalytic reactions and flow-based techniques

SHINSUKE OHNO

The Graduate School of Engineering
Aichi Institute of Technology
(Doctor course)

March 2006

Contents

Chapter 1 Introduction

Most of heavy metals dissolved in environmental water may cause the harmful effect for organism directly or indirectly because of inhibition to the important enzymes in the living systems. The tolerable concentration level on toxic metals is around single ppb. Therefore, the highly sensitive analytical methods for the determination of metal ions at trace levels in environmental waters are required to investigate the water pollution and toxicity. Numerous methods for the analysis of metal ions have been presented; inductively coupled plasma atomic emission spectrometry (ICP-AES), inductively coupled plasma mass spectrometry (ICP-MS), neutron activation analysis (NAA), electrothermal atomization atomic absorption spectrometry (ETAAS) and so on. But these instruments are extremely expensive and the special skill is desired. Thus, the highly sensitive analytical methods that utilize the simple and cost-performance instrument are demanded. Although the conventional spectrophotometries with sensitive chromogenic reagents have been reported in the various fields, it was difficult to analyse metals at single ppb level. The catalytic reaction with the redox is useful for the trace analysis of some metals.

The principles of catalytic reactions are as follows;

$$Red + Ox \rightarrow P + Red_1 \qquad (1)$$

$$Red + M^{n+} \rightarrow P + M^{(n-1)+} \qquad (2)$$

$$M^{(n-1)+} + Ox \rightarrow M^{n+} + Red_1 \qquad (3)$$

,where Red is the reductant, Ox; the oxidant, P; the product, Red_1; the reduced form of Ox and M; the metal ion.

The redox reaction of Red with Ox is proceeded to form P and Red_1 (Equation (1)). This reaction is usually very slow. When M^{n+} is added in the

solution, M^{n+} acts as a catalyst and the oxidation reaction of Red is accelerated (Equation (2)). The reduced $M^{(n-1)+}$ is oxidized again to M^{n+} by Ox (Equation (3)). The product, P, is catalytically produced in the presence of M. As the catalytic reaction occurs cyclically, M concentration at sub nanogram level can be determined by measuring the amount of P. Recently, catalytic methods using the redox catalyst of metals have been proposed for the trace analyses of metals.[1] For example, the metal ions such as Cu(II),[2] Fe(II,III),[3] Mn(II),[4] and Co(II)[5] were determined sensitively. Since these procedures are manual and tedious, automatic detection systems are desired for monitoring metals in water pollutant and material quality in the industry.

Water-soluble compounds such as 2-(5-bromo-2-pyridylazo)-5-[*N*-*n*-propyl-*N*-(3-sulfopropyl)amino]aniline (5-Br-PSAA) and 2-(5-nitro-2-pyridylazo)-5-(*N*-propyl-*N*-sulfopropylamino)phenol (nitro-PAPS) have been proposed as highly sensitive chromogenic reagents, in which sulfoalkyl functional groups were introduced on the para position to the azo group of the heterocyclic-azo-aniline or phenol structures. Since these compounds form a charged quinine structure, their molar absorptivities are large (about 100,000 1 mol^{-1} cm^{-1}) compared with other chelates. Consequently, it can be applied to the spectrophotometric determination of trace amount of heavy metal ions such as Fe(II), Co(III), Ni(II), and Cu(II) and to multi elements analysis by high performance liquid chromatography.

Flow injection analysis (FIA) has been reported by J. Ruzicka and E. H. Hansen in 1975[6,7] as an automatic analytical method. The basic flow system is shown in Fig.1-1. The carrier and reagent solutions are propelled to make a baseline by a pump (P). A sample is injected to the carrier solution via a six-way valve. Then the carrier solution including a sample

solution is mixed with the reagent solution in the reaction coil (RC), and the color development occurs in the coil. Finally, the formed product is measured in a spectrophotometric detector (D).

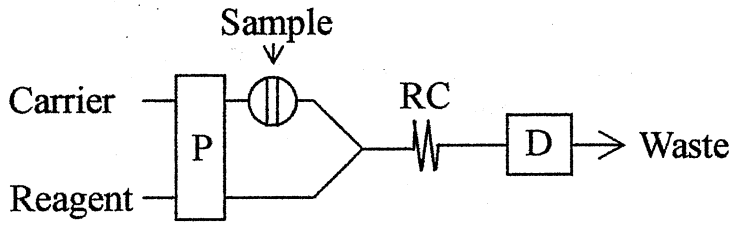

Fig. 1-1 The basic flow system

FIA has some advantages on rapidity, simplicity, and reduction of reagent amounts consumed in the experiment and small sample volume. In the last few decades, many reports on FIA for the determination of organic compound, and metal ions have been published in the various fields. FI techniques with the easy assembly and cost-performance are useful for continuous monitoring in environmental fields, however, it is difficult to analyse multi elements simultaneously. Recently, Sakai et al. reported the multi channel flow cells for the simultaneous determination of metal ions.[8-11] However, the limit of detection was around 1 ppb. To enhance the sensitivity and selectivity for the copper and iron determination, FIA coupled with multi-channel flow cells and catalytic reaction caused by metals was investigated in the proposed methods.

Reactions used in the potentiometric titration have large equilibrium constants around the equivalence point. It is known that a complexing agent changes the potential of a redox reaction involving the metal ions[12] even if the difference in the potential are small. This phenomenon has a potential capacity for the development of novel redox systems. For example, Co(II) can not reduce Fe(III) to Fe(II). But this oxidation reaction

can be proceeded in the presence of nitro-PAPS that can form complexes with Fe(II) and Co(III).

On the other hand, Ruzicka *et al.* have proposed the concept of a sequential injection analysis (SIA) to enhance the potential of flow-based technique.[7,13] The general manifold of SIA is illustrated in Fig.1-2.

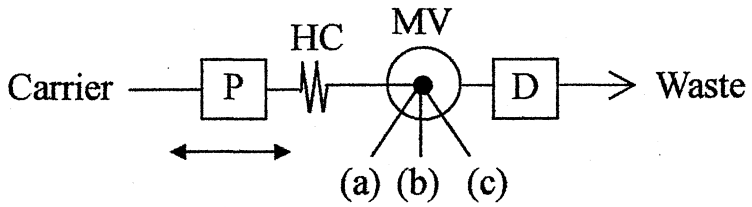

(a) and (b); Reagent, (c); Sample, MV; Multiposition valve, P; Pump, D; Detector, HC; Holding coil

Fig.1-2 The general SIA system

The multiposition valve (MV) is connected to the sample and reagent reservoirs. When the sample and reagents are sequentially drawn into the holding coil (HC) by the pump (P), and then the product formed in HC is forwarded with the carrier to the detector (D). SIA has the advantage on the introduction of some chemical reactions without reconfiguration of the manifold. Beside, the sequence and reaction time can control by the program. Some applications with SIA were reported as the automatic analysis.[14-18] However, there are no reports on the simultaneous determination of metals. In this paper, SIA-LOV (Lab-On-Valve) technique[19] was investigated for the simultaneous analysis of copper and iron by one cycle program.

Chapter 2 Utilization of activating and masking effects by ligands for highly selective catalytic spectrophotometric determination of copper and iron in natural waters[20]

2.1. Introduction

Copper and iron are widespread in the environment and play important roles as essential elements in biological systems. Martin and Fitzwater[21] reported that the addition of nano-molar amounts of iron resulted in an increase of the chlorophyll production by phytoplankton in the open Pacific Ocean. Trace amounts of copper are also required for the phytoplankton production.[22] On the other hand, the toxicity of copper to a brook trout (*Salvelinus fontinalis*) can be greatly diminished when complexing agents such as nitrilotriacetic acid and ethylenediamine tetraacetic acid are added. [23] Such findings indicate that the analyses of trace amounts of copper and iron in natural waters provide significant information regarding biogeochemistry and toxicology. Accordingly, advanced methodology for successive determination of these two ions is of importance.

Kinetic analytical methods based on catalyzed reactions have been applied to trace analyses for various elements because of excellent sensitivity.[24,25] Crouch *et al*[26]. reviewed recent catalytic methods. Kawakubo *et al.* have proposed a catalytic method for speciation of iron in river, tap[27] and rainwater[28] samples, using an iron-catalyzed oxidation reaction of *o*-phenylenediamine with hydrogen peroxide. In the last decade, several workers have reported catalytic methods for binary metal mixtures such as silver(I)-mercury(II),[29] chromium(VI)-tungsten(VI),[30]

iron(II)-antimony(III),[31] molybdenum(VI)-tungsten(VI)[32-35] and osmium(VIII)-ruthenium(IV).[36] A catalytic simultaneous determination of iron, silver and manganese with stopped-flow injection was reported.[37] These metals have different catalytic effects on the oxidation of Rhodamine B by periodate in the presence of 1,10-phenanthroline (phen) as an activator. The analysis of a single species is popular on the catalytic method, however, there are few reports on a catalytic method for the simultaneous and/or successive determination of copper and iron, which is based on the effects of selective activators for their catalytic actions.

Kawashima *et al.* reported that copper(II)[38] and iron(III)[39] catalyzed the oxidative coupling reaction of *p*-anisidine and *N,N*-dimethylaniline (DMA) in the presence of hydrogen peroxide. The use of activators in catalytic methods allows an increase in the sensitivity and an improvement in the selectivity as well.[24,25,40] Recently, Teshima et al.[41] reported a short communication concerning a new catalytic flow-injection method for the successive determination of copper and iron. It was based on the effects of activators such as 2,9-dimethyl-1,10-phenanthroline(neocuproine) and phen on the copper- and iron-catalyzed oxidative coupling reaction of *p*-anisidine with DMA. In this study, the detailed analytical conditions by the batchwise procedure were investigated, and the proposed method was applied to the determination of copper and iron in natural waters.

2.2. Experimental

All reagents were of analytical-reagent grade and were used without further purification. All solutions were prepared with deionized water purified with an Advantec Aquarius GSH-210 system. The descriptions

mentioned above are commonly used in Chapters 3, 4 and 5.

2.2.1. Reagents

A commercially available 100 ppm copper(II) and iron(III) standard solutions for atomic absorption spectrophotometry (Wako, Osaka) were used. Working solutions of copper and iron were prepared by suitable dilution of standard solutions with 0.01 M hydrochloric acid, respectively.

A 0.1 M *p*-anisidine solution was prepared by dissolving 3.08 g of *p*-anisidine (Wako, Osaka) in 70 ml of 4 M hydrochloric acid and made up to 250 ml with water.

A 0.2 M DMA solution was prepared by dissolving 6.06 g of *N,N*-dimethylaniline (Wako, Osaka) in 20 ml of 4 M hydrochloric acid and made up to 250 ml with water.

A 5 M hydrogen peroxide solution was prepared by diluting 25 ml of commercial 30 % hydrogen peroxide (Sigma Aldrich Japan, Tokyo) to 50 ml with water.

A 4×10^{-3} M neocuproine solution was prepared by dissolving 0.245 g of neocuproine hydrochloride (Tokyo Kasei, Tokyo) with 250 ml of water.

A 5×10^{-3} M phen solution was prepared by dissolving 0.099 g of 1,10-phenanthroline monohydrate (Dojindo Laboratories, Kumamoto) in 4 ml of 1 M hydrochloric acid and made up to 100 ml with water.

A 2.5×10^{-2} M diphosphate solution was prepared by dissolving 1.12 g of sodium diphosphate decahydrate (Wako, Osaka) with 250 ml of water.

A 1.25 M acetic acid solution was prepared by diluting 19 ml of acetic acid (Sigma Aldrich Japan, Tokyo) to 250 ml with water. A 1.25 M sodium acetate solution was prepared by dissolving 17.0 g of sodium acetate

trihydrate (Nakarai Tesque, Kyoto) with water and made up to 100 ml with water. These two solutions were mixed to prepare a buffer solution (pH 3.2).

A bathocuproinedisulfonate solution was prepared by dissolving appropriate amounts of bathocuproinedisulfonic acid, disodium salt (Dojindo Laboratories, Kumamoto) with water.

A bathophenanthrolinedisulfonate solution was prepared by dissolving appropriate amounts of bathophenanthrolinedisulfonic acid, disodium salt (Dojindo Laboratories, Kumamoto) with water.

2.2.2. Apparatus

A U-2000A double-beam spectrophotometer was used with 10 mm light-path cells for absorbance measurements. A Horiba Model F-22 pH/mV meter was used for pH adjustment. A Taiyo Kagaku Kogyo C-630 thermostat was used to maintain reaction temperature.

2.2.3. Procedure for copper determination

To 2.5 ml of 0.1 M p-anisidine in a 25 ml of volumetric flask, 2.5 ml of 0.2 M DMA, 2 ml of 1.25 M acetate buffer, 2 ml of 2.5×10^{-2} M diphosphate, an appropriate amount of copper (4～250 ng) and 2.5 ml of 4×10^{-3} M neocuproine were added. Then after adjusting pH 3.2 with 1 M sodium hydroxide solution, the solution was kept at 55℃ in a thermostated bath for about 5 min to attain thermal equilibrium. To initiate the catalytic reaction, a 2.5 ml of 5 M hydrogen peroxide heated at 55℃ was added, and diluted to the mark with water. At 5 min after the initiation of the

reaction, a portion of the sample solution was immersed in an ice bath about 30 second for quenching. The increase in absorbance was measured at 740 nm against a water reference.

2.2.4. Procedure for iron determination

To the same reagents as described above, 25~2500 ng of iron and 2.5 ml of 5×10^{-3} M phen were added. The reaction temperature at 60℃ and reaction time for 15 min were used for the iron determination.

2.3.. Results and Discussion

Copper(II) and iron(III) catalyze the oxidative coupling of *p*-anisidine with DMA to form a colored compound, which has a maximum absorption wavelength at 740 nm. This reaction is shown in Scheme 2-1.

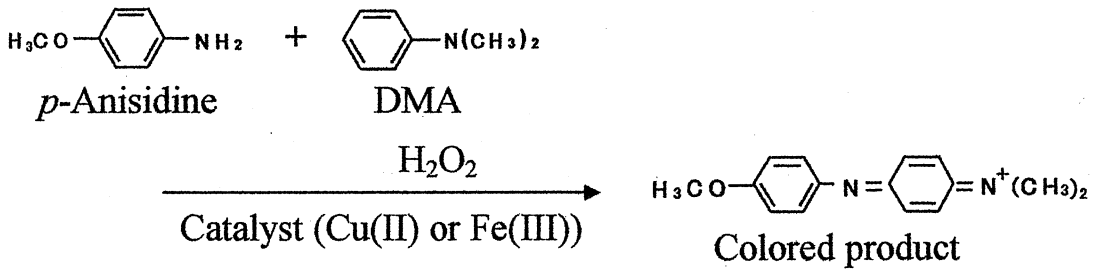

Scheme 2-1

These spcetra are shown in Fig. 2-1 (a) for copper and (b) for iron. The reaction occurred in the presence of hydrogen peroxide at pH 3.2. In the indicator reactions, neocuproine was added as an activator to the determination of copper, and phen for iron was added as the activator. The experimental variables such as reaction pH, reaction time, reaction

temperature and reagents concentrations were optimized in order to achieve highly sensitivity and selectivity on the determination of copper and iron.

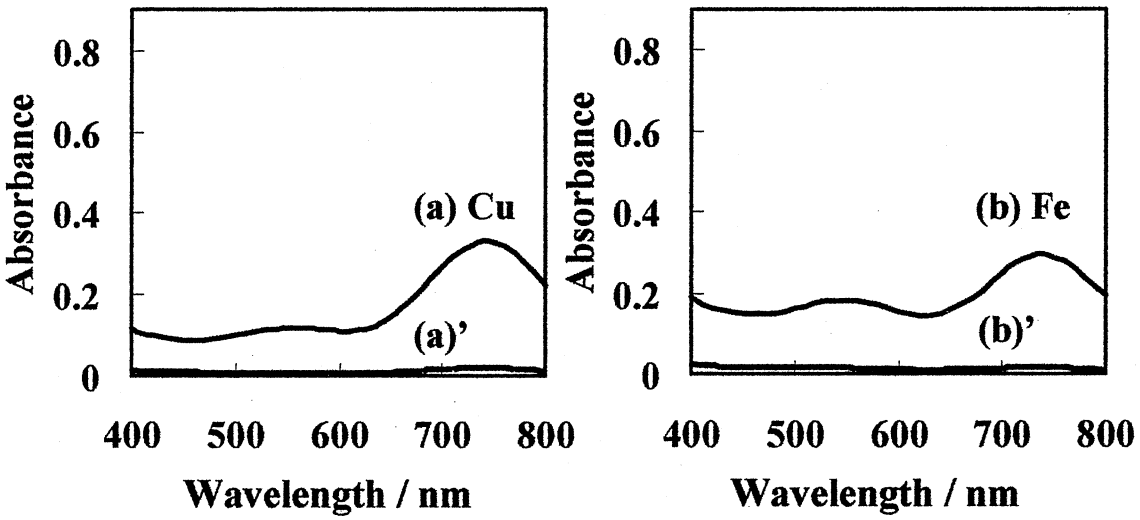

Fig. 2-1 Absorption spectra on the metal catalyzed ((a),(b)) and uncatalyzed ((a)',(b)') reactions. (a), 10 ppb copper, $C_{\text{neocuproine}}$ = 0.0004 M, reaction time = 5 min, reaction temperature = 55℃; 40 ppb iron, C_{phen} = 0.0005 M, reaction time = 15 min, reaction temperature = 60℃. Others: $C_{p\text{-anisidine}}$, 0.01 M; C_{DMA}, 0.02 M; $C_{\text{Acetate buffer}}$ 0.1 M (pH 3.2); $C_{\text{diphosphate}}$, 0.002 M; $C_{\text{hydrogen peroxide}}$; 0.5 M.

2.3.1. Effects of activators

The choice of suitable activators in catalytic methods permits the improvement in their sensitivity and selectivity. The concentration effects of several polypyridines such as neocuproine, bathocuproinedisulfonate (BCS), phen and bathophenanthrolinedisulfonate (BPS) on the uncatalyzed and copper- and iron-catalyzed dye-forming reactions were investigated. The concentrations were varied in the range from 0 to 2×10^{-3} M.

Fig. 2-2 shows the effects of neocuproine and BCS concentrations. The catalytic activity of copper was activated by adding neocuproine and/or

BCS, while these two ligands had no effect on the iron-catalyzed reaction. Therefore, in the presence of neocuproine or BCS, copper can be determined selectively. The absorbance of the copper-catalyzed reaction increased with increasing neocuproine (or BCS) concentration up to 4×10^{-4} M (1×10^{-4} M for BCS) and then decreased gradually over 8×10^{-4} M (2×10^{-4} M for BCS). Such dependence is a characteristic feature for the types of activated reactions when the activator is concerned with the formation of

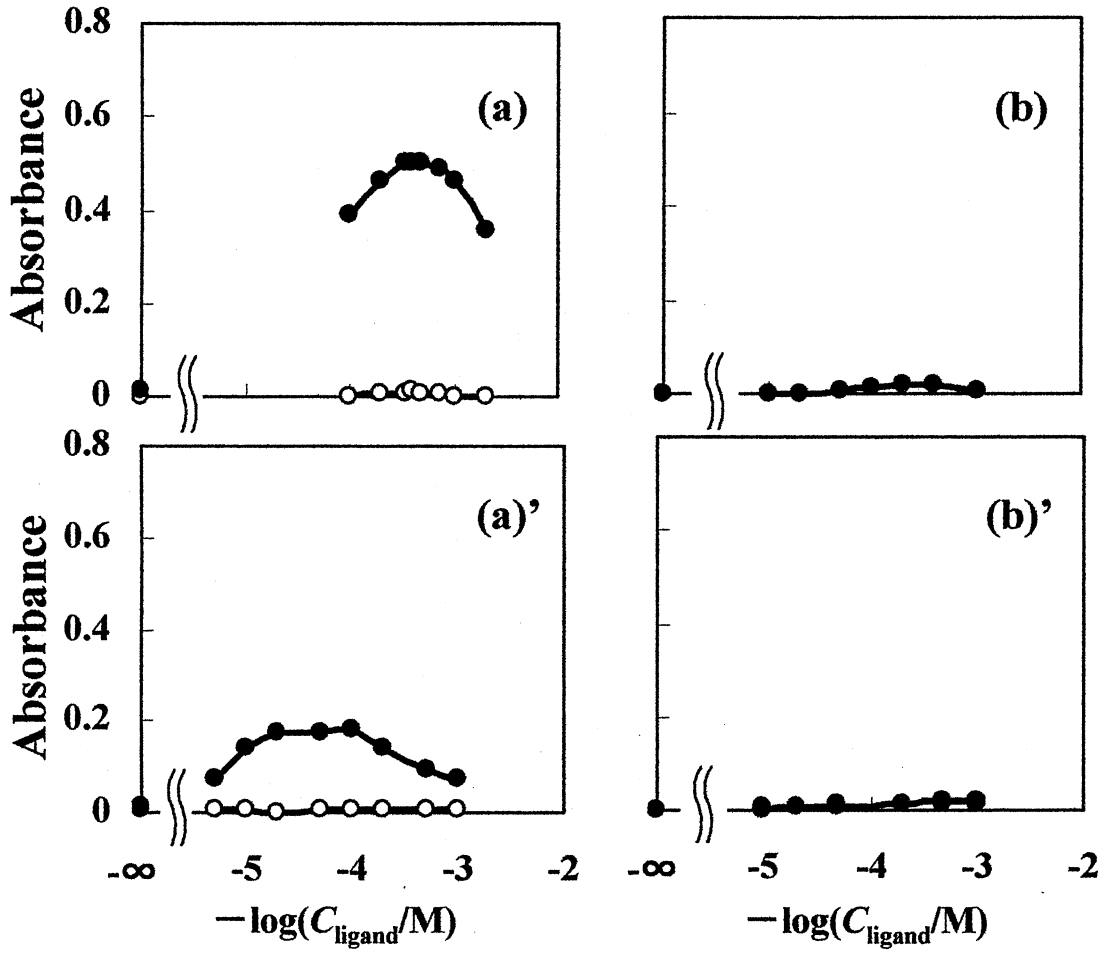

Fig. 2-2 Effects of neocuproine ((a),(b)) and BCS ((a)',(b)') concentrations on the uncatalyzed (○) and metal catalyzed (●) reactions. Other conditions as in Fig. 2-1.

ternary complexes of the activator-metal-substrate[40]: neocuproine- (or BCS-) copper-*p*-anisidine and/or DMA. The coordination sphere of the

catalyst is fully occupied by the activator and any complexation with the substrate does not occur at higher concentrations of activator.[25] The effect of neocuproine was greater than that of BCS. A 4×10^{-4} M neocuproine concentration was selected for the copper determination.

The effects of phen and BPS concentrations for iron are shown in Fig. 2-3.

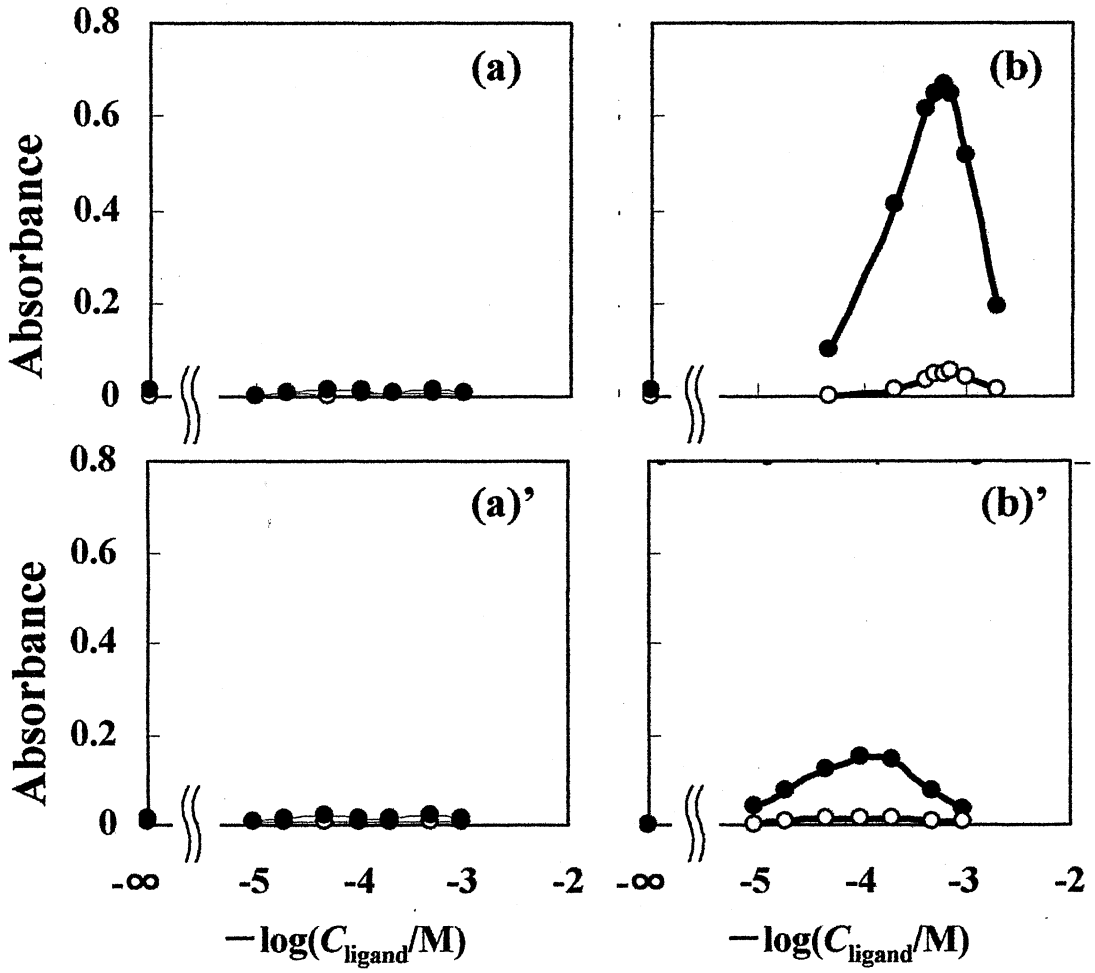

Fig. 2-3 Effects of phen ((a) , (b)) and BPS ((a)' , (b)') concentrations on the uncatalyzed (○) and metal catalyzed (●) reactions. (a) and (a)', 10 ppb copper; (b) and (b)', 40ppb iron. Other conditions as in Fig. 2-1.

The catalytic activity of iron was activated in the presence of phen and BPS, but that of copper was not observed. The absorbance for the iron-catalyzed reaction increased with increasing phen (or BPS) concentration, however, over 7×10^{-4} M (2×10^{-4} M for BPS), the absorbance decreased. It seems that the formation of ternary complexes of the phen- (or BPS-) iron-*p*-anisidine and/or DMA were restricted in higher phen and BPC concentration ranges. A maximum absorbance was obtained at 5×10^{-4} M phen.

The conditional redox potentials of Cu(II)/Cu(I) and Fe(III)/Fe(II) systems increase in the presence of neocuproine and phen, because the stability constant of copper(I)-neocuproine complex ($\log\beta_2 = 19.1$) is larger

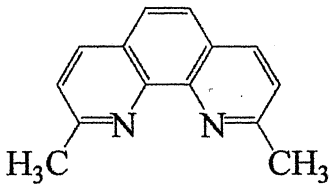

Neocuproine

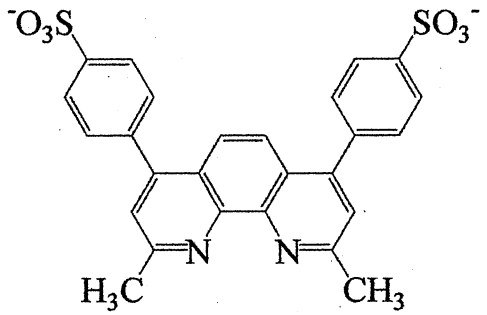

Bathocuproine-di-sulfonate(BCS)

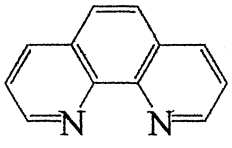

Phen

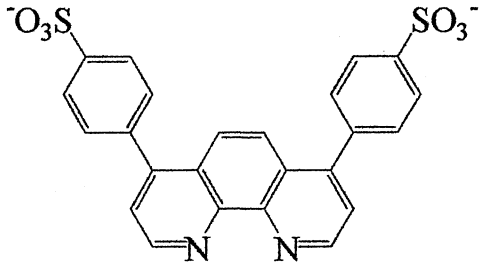

Bathophenanthroline-di-sulfonate (BPS)

Fig. 2-4 Structures of polypyridines

than that of the copper(II)-neocuproine complex ($\log\beta_2$ = 11.7) and also that of the iron(II)-phen complex ($\log\beta_3$ = 21.3) is greater than that of iron(III)-phen complex ($\log\beta_3$ = 14.1).[42] In the indicator reaction system, neocuproine and phen, which increase the oxidizing powers of copper(II) and iron(III), acted effectively for copper and iron catalysts. Fig. 2-4 shows polypyridines investigated in this study.

2.3.2. *Effect of diphosphate concentration*

In the previous paper,[41] it was found that the catalytic action of iron on the dye-forming reaction disappeared in the presence of the Britton-Robinson buffer solution, which consisted of acetic, phosphoric and boric acids because iron(III) was masked by phosphate. In this study, the effect of diphosphate was tested to enhance the selectivity for copper and iron.

Table 2-1 shows the result of recovery test with and without diphosphate. In the absence of diphosphate, the recovery of copper was over 100% because of a positive interference of iron. The recovery of iron was less than 100%. This reason was probably related to the formation of copper(II)-phen complex ($\log\beta_3$ = 20.9)[42], *i.e.*, the activating effect of phen

Table 2-1 Recoveries of copper and iron without and with diphosphate

Cu added / ppb	Fe added / ppb	Cu found / ppb		Fe found / ppb	
		Without	With	Without	With
2	50	10.5 (524)[a]	1.99(100)[a]	48.8 (98)[a]	51.7 (103)[a]
5	50	13.7 (274)[a]	4.74 (95)[a]	45.6 (91)[a]	50.9 (102)[a]
10	50	17.3 (173)[a]	9.86 (99)[a]	44.1 (88)[a]	52.0 (104)[a]
10	20	14.6 (146)[a]	9.56 (96)[a]	18.0 (90)[a]	20.9 (105)[a]
10	100	19.9 (199)[a]	10.2 (102)[a]	117 (117)[a]	94.9 (95)[a]

[a] Recovery (%) =: $\frac{\text{Found}}{\text{added}} \times 100$:

on the iron catalysis was inhibited. On the other hand, the recoveries of both elements were improved in the presence of diphosphate.

Fig. 2-5 (a) shows the effect of diphosphate concentration on the uncatalyzed and copper-catalyzed dye-forming reactions. In the absence of diphosphate, the highest absorbance for the copper-catalyzed reaction was obtained (-∞), but the absorbance of the uncatalyzed one was also high. In the presence of diphosphate, the catalytic action of copper was depressed because of the masking of copper with diphosphate ($\log\beta_2 = 10.3$).[43] A part of copper ion acted as a catalyst by adding neocuproine. A constant absorbance in the copper-catalyzed reaction was obtained in the concentration range from 2×10^{-4} to 5×10^{-3} M, and the blank absorbance was quiet low in the above range. Fig. 2-5 (b) shows the effect of diphosphate concentration on the uncatalyzed and iron-catalyzed reactions.

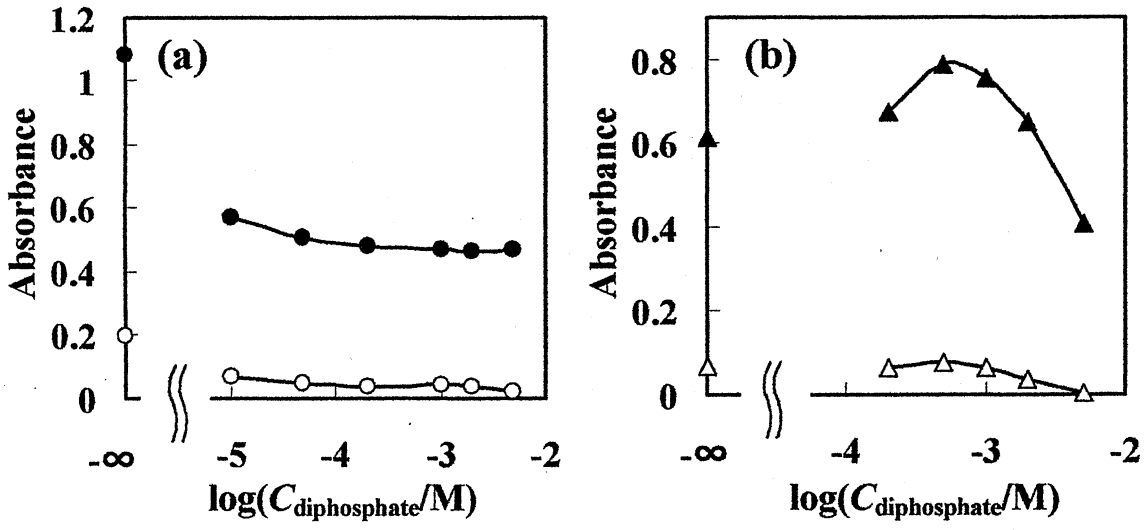

Fig. 2-5 Effects of diphosphate concentration on the uncatalyzed ((△) for 15 min, (○) for 5 min) and catalyzed ((▲) for 15 min, (●) for 5 min) reactions. (a), 10 ppb copper; (b), 100 ppb iron. Other conditions as in Fig. 2-1.

The reaction times were 5 and 15 min. At 5 min, iron was masked with increasing the diphosphate concentration. At 15 min, the masking effect was observed above 1×10^{-3} M, and also the absorbance of the uncatalyzed reaction decreased above this concentration. A 2×10^{-3} M diphosphate was selected for each element determinations.

2.3.3. *Effects of reaction temperature and time*

The effects of reaction temperature and time on the dye formation were studied. The results are shown in Fig. 2-6. The copper-catalyzed reaction proceeded faster with an increase in temperature. When temperature was above 50℃, the absorbance decreased because the produced dye was decomposed. Since constant absorbance was obtained in the range from 4 to 7 min at 55℃, the reaction temperature and time were set at 55℃ and 5 min for the copper determination. Similarly, an increase in temperature gave the larger absorbance in the iron-catalyzed reaction. When the

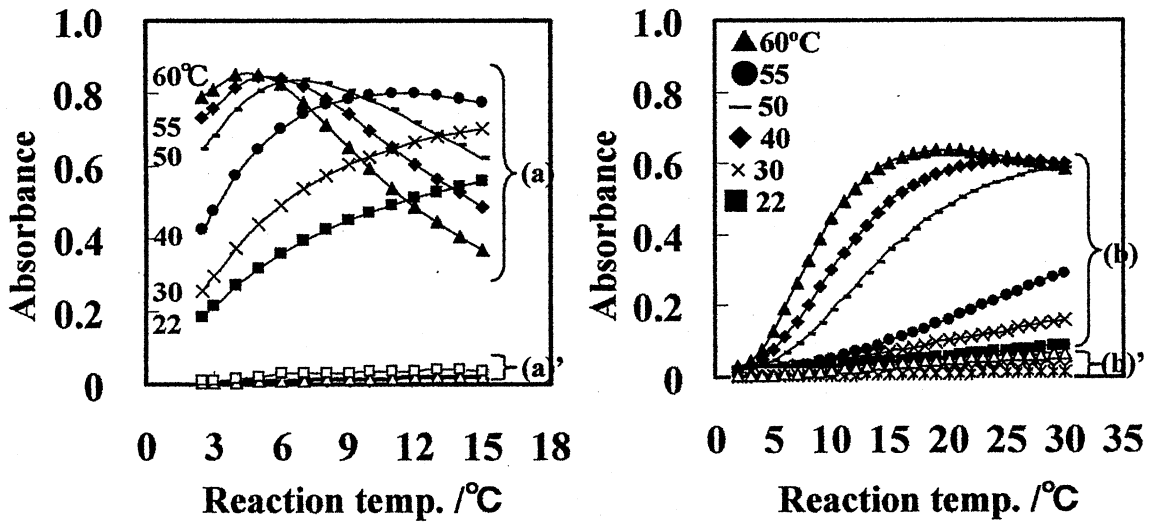

Fig. 2-6 Effects of reaction temperature on the dye-formation. (a) and (a)', 50 ppb copper and blank for copper determination; (b), and (b)', 50 ppb iron and blank for iron determination. Conditions as in Fig. 2-1.

temperature was set at 60℃, the decomposition of the dye was observed over 20 min. The iron determination was carried out at 60℃ and 15 min.

2.3.4. *Effects of other variables*

The pHs of the copper- and iron-catalyzed reaction systems were varied from 1.5 to 4 (Fig. 2-7). A maximum absorbance was obtained at pH 3.2 for each. Thus, both catalytic reactions were carried out at pH 3.2.

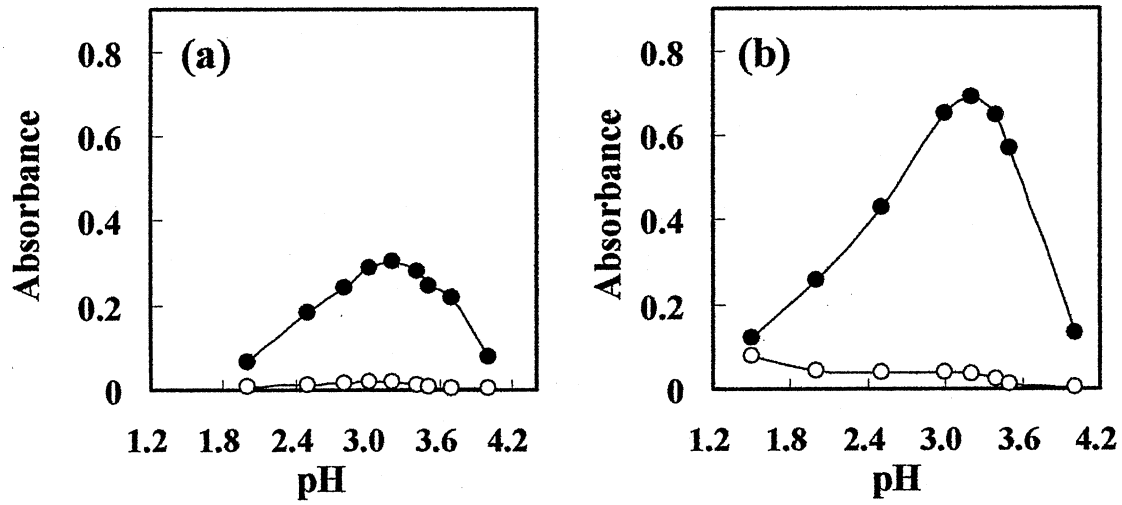

Fig. 2-7 Effects of pH on the uncatalyzed (○) and catalyzed (●) reactions. (a), 4 ppb copper; (b), 50 ppb iron. Other conditions as in Fig. 2-1.

The effects of other reagent concentrations on the uncatalyzed and copper-catalyzed dye-forming reactions were studied. The *p*-anisidine concentration was varied from 0 to 2×10^{-2} M. The absorbance increased with increasing the concentration up to 1×10^{-2} M, and was constant over 1×10^{-2} M. A 1×10^{-2} M *p*-anisidine concentration was selected. The DMA concentration was varied from 0 to 3×10^{-2} M. A constant absorbance was

obtained in the range from 1.5×10^{-2} to 3×10^{-2} M. A 2×10^{-2} M DMA was used. The effect of hydrogen peroxide concentration was examined in the range from 0 to 0.8 M. The absorbance was maximal and constant over the concentration of 0.3 M. In this study, a 0.5 M hydrogen peroxide was selected. The acetate buffer concentration was varied from 4×10^{-2} to 0.4 M. The absorbance was constant in the range from 0.1 to 0.4 M. Absorbance of the reagent blank slightly increased with an increase in the concentration. A 0.1 M acetate buffer was thus selected.

2.3.5. Calibration graphs

Calibration graphs for copper and iron were prepared under the optimum conditions described above. The results are shown in Fig. 2-8. Although two graphs slightly displayed downward curvature, the repeatability by the

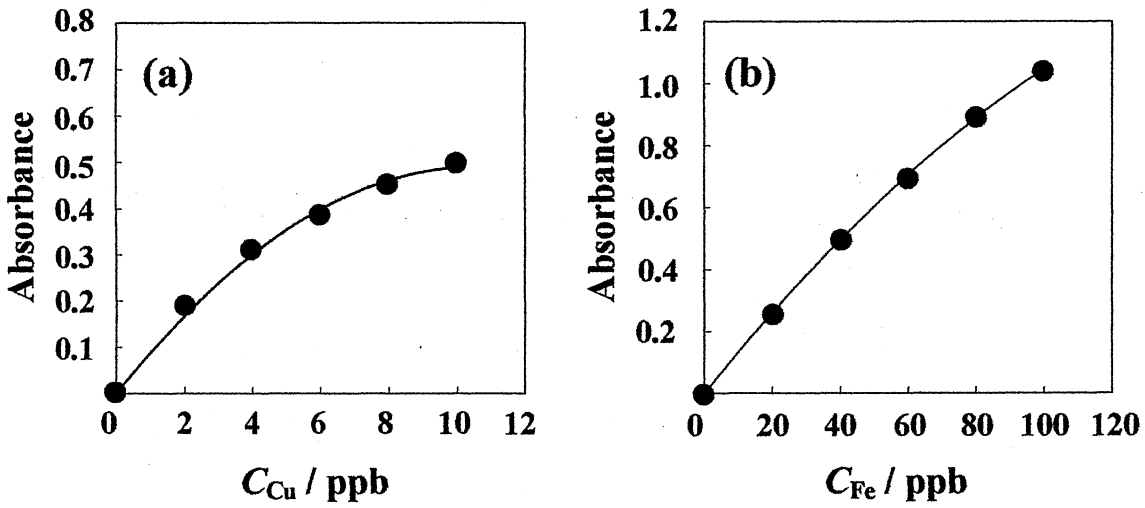

Fig. 2-8 Calibration curves for (a) copper and (b) iron. Other conditions as in Fig. 2-1.

proposed method was satisfactory with low relative standard deviations (n = 5) of 1.1% for 10 ppb copper and 0.97% for 40 ppb iron. The determinable ranges were 0.16 – 10 ppb for copper and 1 – 100 ppb for iron. The detection limits (3σ) for copper and iron were 0.05 ppb and 0.3 ppb, respectively.

The successive determinations of copper and iron in artificial mixtures were carried out at various concentration ratios. The result is shown in Table 2-2. The concentration ranges were 1-10 ppb copper and 10-200 ppb iron, respectively. An error of $\pm$5% was considered to be tolerable. The accurate result for 1 ppb copper was obtained when 200 ppb iron was coexisted. On the other hand, the presence of 10 ppb copper was tolerable in the determination of 20 ppb iron.

Table 2-2 Successive determinations of copper and iron in artificial mixtures

Added/ppb		Found/ppb		Recovery/%	
Cu	Fe	Cu	Fe	Cu	Fe
1	10	0.97	9.91	97	99
1	100	1.03	104	103	104
1	200	1.04	-	104	-
2	50	1.99	51.7	100	103
2	100	2.10	97.6	105	98
2	200	2.06	-	103	-
5	50	4.74	50.9	95	102
5	100	5.14	98.1	103	98
5	200	5.26	-	105	-
10	20	9.56	20.9	96	105
10	50	9.86	52.0	99	104
10	100	10.2	94.9	102	95
10	200	10.4	-	104	-

2.3.6. *Interference study*

The effects of foreign ions on the determination of 4 ppb copper and 20 ppb iron in the mixture were studied. The results are summarized in Table 2-3. An error of ±5% was considered to be tolerable. Most ions gave no interference on the determination of copper and iron in concentrations up to at least 200 ppb. A 200 ppb nickel(II) gave a positive interference on the determination of copper. It seems that nickel(II) acted as a catalysis on the dye-forming reaction, but 50 ppb nickel(II) was tolerable. The concentration levels of these ions listed in Table 2-3 are generally tolerable when the method is applied to natural waters.

Table 2-3 Effects of diverse ions on the determination of a mixture of 4 ppb Cu and 20 ppb Fe

Tolerance limit / ppb	For Cu determination	For Fe determination
50000	Na(I), K(I), Mg(II), Ca(II), NO_3^-, Cl^-, SO_4^{2-}, BO_3^{3-}	Na(I), K(I), NO_3^-, Cl^-, SO_4^{2-}, BO_3^{3-}
20000	Al(III)	Mg(II), Ca(II)
2000	Cd(II)	Al(III), Zn(II), Pb(II)
1000	Pb(II)	Cr(VI), Cd(II)
500	Mn(II)	
200	Cr(VI), Co(II), Zn(II)	Mn(II), Co(II), Ni(II)
50	Ni(II)	

2.3.7. *Application to natural waters*

To validate the proposed method, the technique was applied to the determination of copper and iron in a standard river water (JAC 0032) purchased from Japan Society of Analytical Chemistry. A 2.5 ml of the river water was put into a 25 ml volumetric flask and other reagents were

added. As shown in Table 2-4, the analytical values obtained by the method are in good agreement with the certified values.

Tap water and natural waters such as well, river and pond samples were analyzed by the proposed method. The tap water sample was acidified by adding concentrated hydrochloric acid to pH about 2. The natural water samples were filtered through a Millipore membrane filter (0.45 μm pore size) and acidified to pH about 2 in the same manner. The analytical results of the tap and natural waters are summarized in Table 2-5. The recoveries of added copper and iron were found to be quantitative and the reproducibility was also satisfactory.

Table 2-4 Determination of copper and iron in the standard river water(in spiked)[a]

Sample	Found / ppb		Certified values / ppb	
	Cu[b]	Fe[b]	Cu	Fe
JAC 0032	10.4 ±0.2[c]	63.0 ±1.0[c]	10.5 ±0.2	57 ±2
	10.5 ±0.2[d]	58.3 ±1.2[d]	10.5 ±0.2	57 ±2

a : Purchased from Japan Society of Analytical Chemistry.
b : Average for 3 determinations.
c : The river water was diluted 5 times.
d : The river water was diluted 10 times.

Table 2-5 Determination of copper and iron in tap and natural waters

Sample	Taken / ml		Added/ppb		Found/ppb		In sample/ppb		Recovery, %	
	Cu	Fe	Cu	Fe	Cu	Fe	Cu	Fe	Cu	Fe
Tap	10	5	0	0	0.67	9.46	1.68	47.3	-	-
	10	5	1	10	1.72	20.0	1.80	50.0	105	105
	10	5	2	20	2.72	29.8	1.80	49.0	103	102
	10	5	3	30	3.65	39.5	1.63	47.5	99	100
							Ave.1.73±0.09	48.5±1.28		
Well	5	2.5	0	0	1.17	38.1	5.85	381	-	-
	5	2.5	1	10	2.17	48.2	5.85	382	100	101
	5	2.5	2	20	3.13	57.7	5.65	377	98	98
	5	2.5	3	30	4.01	66.7	5.05	367	95	95
							Ave.5.60±0.38	377±6.85		
River	10	5	0	0	0.49	43.8	1.23	219	-	-
	10	5	1	10	1.45	53.3	1.13	217	96	95
	10	5	2	20	2.43	64.3	1.08	222	97	103
	10	5	3	30	3.52	72.3	1.30	212	101	95
							Ave.1.18±0.10	217±4.27		
Pond	10	5	0	0	0.22	6.69	0.55	33.5	-	-
	10	5	1	10	1.27	16.9	0.68	34.5	105	102
	10	5	2	20	2.31	26.8	0.78	34.0	105	101
	10	5	3	30	3.27	37.6	0.68	38.0	102	103
							Ave.0.67±0.09	35.0±2.05		

2. 4. Conclusion

A selective and sensitive spectrophotometric method was proposed for the successive determination of trace amounts of copper and iron. The method is based on the catalytic effects of copper and iron on the oxidative coupling reaction of *p*-anisidine with DMA in the presence of hydrogen peroxide. The selectivity and sensitivity of the proposed method were greatly enhanced by adding neocuproine and phen as activators and diphosphate as the masking agent. The method was successfully applied to the analyses of copper and iron in tap and natural waters without preconcentration and separation.

Chapter 3 Flow injection-catalytic photometric methods for ultratrace amounts of copper and/or iron[44, 45]

3.1. Introduction

Trace amounts of copper and iron exist widely in river, tap, pond, well, and underground waters. These metals are essential trace elements for biological systems. Numerous dissolving chemical forms, such as aqua ions, complexes and colloids, are observed in natural water. In general, the toxicity of dissolved copper(II) is considered to be much less than that of mercury, but greater than that of cadmium, silver, lead, and zinc.[46] However, it has been reported that chelating agents, such as nitrilotriacetic acid and ethylenediaminetetraacetic acid, decreased the toxicity of copper.[23] Therefore, it is very important to analyse the complexation reactions of ppb levels of copper and iron with some ligands existing in natural water. However, the concentration levels of these metals existing in natural water are trace and/or ultratrace (single ppb or sub-ppb level). Accordingly, a highly sensitive analytical method for the determination of copper and iron is required to investigate water pollution and toxicology.

Catalytic methods based on catalyzed reactions have been developed for the determination of manganese, chromium, cobalt, vanadium, and copper ions at trace and ultratrace levels.[5,47-50] Kawashima et al. have determined ppb levels of iron in tap and hot-spring water samples.[51] On the other hand, adsorptive cathodic stripping voltammetry (ACSV) was proposed to measure copper in sea water at trace levels.[52] However, one of the major problems in ACSV is the adsorption of organic compounds on the electrode.[53]

The catalytic methods require a strict control of the reaction temperature, time, and constant mixing of the reagents. Flow injection analysis (FIA) is efficient to control serious experimental conditions and the assembly is easy. However, it is difficult to successively determine several analytes by an FIA system equipped with a conventional flow cell. Recently, Sakai and his co-workers designed two-channel double and serial flow cells[8] and a twin flow cell[54] for the simultaneous determination of copper and iron with 2-(5-bromo-2-pyridylazo)-5-[*N*-*n*-propyl-*N*-(3-sulfopropyl)amino]aniline, sodium salt (5-Br-PSAA) or 2-(5-nitro-2- pyridylazo)-5-[*N*-*n*-propyl-*N*-(3-sulfopropyl)amino]phenol, disodium salt, dihydrate (Nitro-PAPS). However, these methods using chromogenic reagents were not sufficient to the determination of sub-ppb levels of copper and iron. During the recent decade, some researchers have reported on catalytic methods for binary metal mixtures, such as silver(I)-mercury(II)[29], chromium(VI)-tungsten(VI)[30], and iron(II)-antimonony(III).[31] However, there are few reports on catalytic methods for the determination of two catalysts using a single indicator reaction.

In the presence of hydrogen peroxide, *p*-anisidine reacted with *N*,*N*-dimethylaniline (DMA) to form a dye (λ_{max} =740 nm). Although the oxidative coupling reaction was slow, the reaction rate was accelerated in the presence of copper(II)[55] or iron(III)[39]. Since the absorbance of the dye formed at a fixed time was proportional to these metal concentrations, it was possible to determine copper(II) and iron(III). In a previous paper,[20] this catalytic analysis was performed to determine copper(II) and iron(III) selectively by a batchwise method. The catalytic reaction with metals is shown in Scheme 3-1.

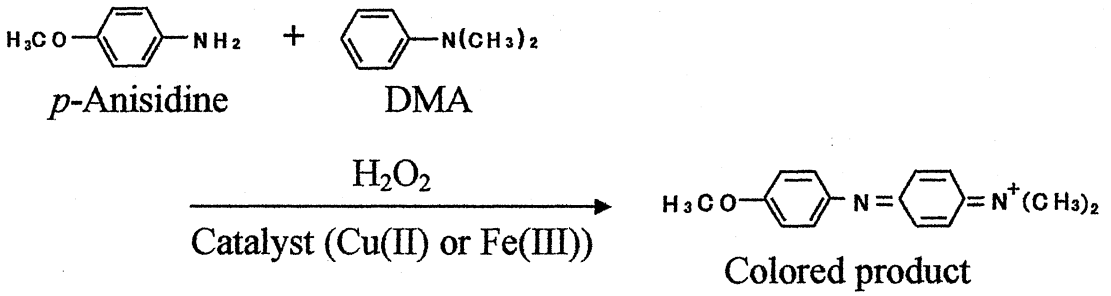

Scheme 3-1

2,4,6-Tris(2-pyridyl)-1,3,5-triazine (TPTZ) reacts with iron(II) to form a purple iron(II)-TPTZ complex (λ_{max} = 593 nm). Recently, the trace determination of copper(II) based on the catalytic effect on the redox reaction of cysteine with iron(III) by FIA in the presence of TPTZ was proposed.[45] The detection limit (3σ) and the determinable range were 0.005 and 0.05 – 8 ppb. The method was successfully applied to the determination of copper in the standard river water sample issued from the Japan Society for Analytical Chemistry and serum samples.

In this chapter, catalytic methods for ultratrace amounts of copper and/or iron using an FIA system are described. The catalytic-FIA method using a serial flow cell can be applied to the successive determination of trace amounts of copper(II) and iron(III), and also to the determination of labile and inert complexes in synthesized samples involving humic acid and copper(II) or iron(III).

3.2. Experimental

3.2.1. Reagents

The copper(II) and iron(III) standard solutions were prepared in the same manner in Chapter 2.

A 0.25 M *p*-anisidine solution was prepared by dissolving 15.4 g of *p*-anisidine (Wako) in 150 ml of conc. hydrochloric acid and made up to 500 ml with water.

A 0.6 M DMA solution was prepared by dissolving 36.4 g of DMA (Wako) in 90 ml of 4 M hydrochloric acid and made up to 500 ml with water.

A 2 M acetic acid solution was prepared by diluting 60 ml of acetic acid (Sigma Aldrich Japan, Tokyo) to 500 ml with water. A 2 M sodium acetate solution was prepared by dissolving 27.2 g of sodium acetate trihydrate (Nakalai Tesque, Kyoto) with water and made up to 100 ml with water. These solutions were mixed to prepare a buffer solution (pH 3.1).

A 0.1 M diphosphate solution was prepared by dissolving 2.23 g of sodium diphosphate decahydrate (Wako) with 50 ml of water.

A 0.25 M 1,10-phenanthroline (phen) solution was prepared by dissolving 4.96 g of 1,10-phenanthroline monohydrate (Dojindo Laboratories, Kumamoto) with 8 ml of 4 M hydrochloric acid.

Hydrogen peroxide solutions (0.5 and 3 M) were prepared by diluting appropriate amounts of 30% hydrogen peroxide with 0.01 M HCl.

3.2.2. Apparatus

Fig. 3-1 shows a schematic diagram of a flow-injection system using a serial flow cell for the successive determination of copper(II) and iron(III). The system consists of two double-plunger pumps (DMX-2000, Sanuki Kogyo, Tokyo and Type DUAL PUMP201, F·I·A Instrument, Tokyo),

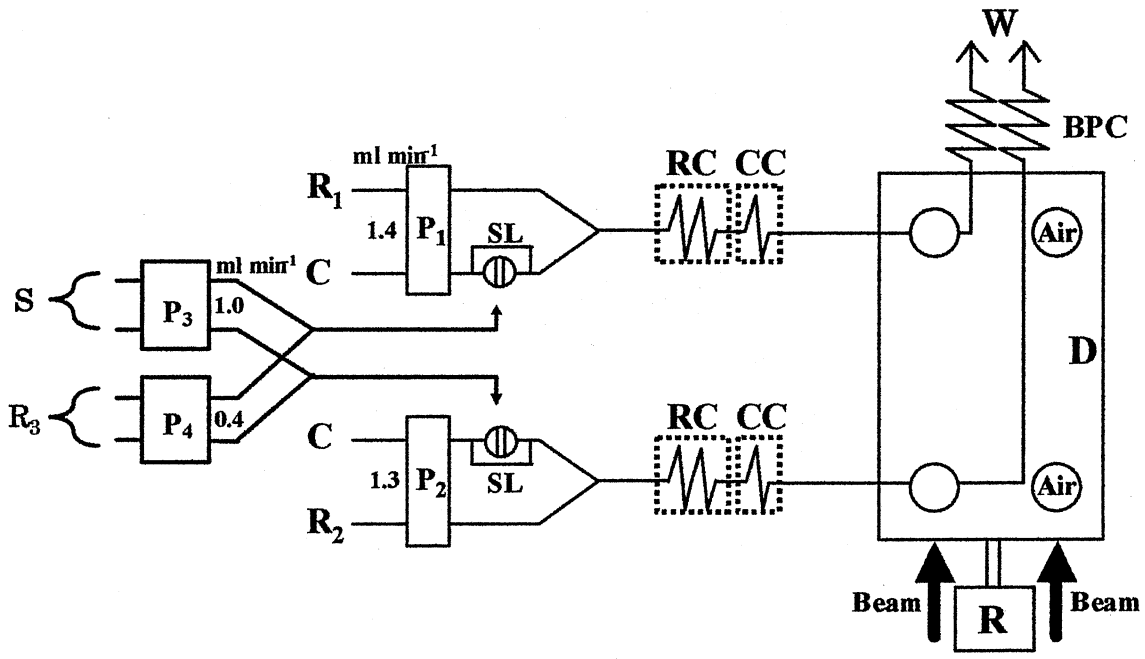

Fig. 3-1 Schematic diagram of a flow-injection system equipped with a serial flow cell. C, carrier solution (0.5 M hydrogen peroxide at pH 2); R_1 (0.08 M *p*-anisidine, 0.06 M DMA, 0.2 M acetate buffer (pH 3.1), 2×10^{-3} M diphosphate); R_2 (0.06 M *p*-anisidine, 0.06 M DMA, 0.2 M acetate buffer (pH 3.1), 2×10^{-3} M diphosphate, 2×10^{-3} M phen); P_1 and P_2, pumps; SL, sample loops (2m× ϕ 0.5 mm); RC, reaction coil (8 m× ϕ 0.5 mm, 90℃); CC, cooling coil (1 m× ϕ 0.5 mm); BPC, back pressure coil (35 cm× ϕ 0.25 mm); D, double beam spectrophotometer equipped with serial flow cell (740 nm); R, recorder; W, waste; S, sample; R_3, 3 M hydrogen peroxide at pH 2; P_3 and P_4, peristaltic pumps.

two six-way injection valves (SVM-6M2, Sanuki Kogyo), two thermostated baths (R-3000C, Sanuki Kogyo and Type 521, F・I・A Instrument), a spectrophotometer (S-3250, Soma Optics, Tokyo) equipped with a serial flow cell (cell volume: 4 μl; path length: 5 mm) [8], two peristaltic pumps (U4-8R, Alitea, Sweden) and a recorder (EB22005, Chino, Tokyo). The configuration of a serial flow cell is shown in Fig. 3-2.

All connecting lines and reaction coils were made from 0.5 mm i.d. Teflon tubing. A Horiba Model F-22 pH/mV meter was used for pH adjustment.

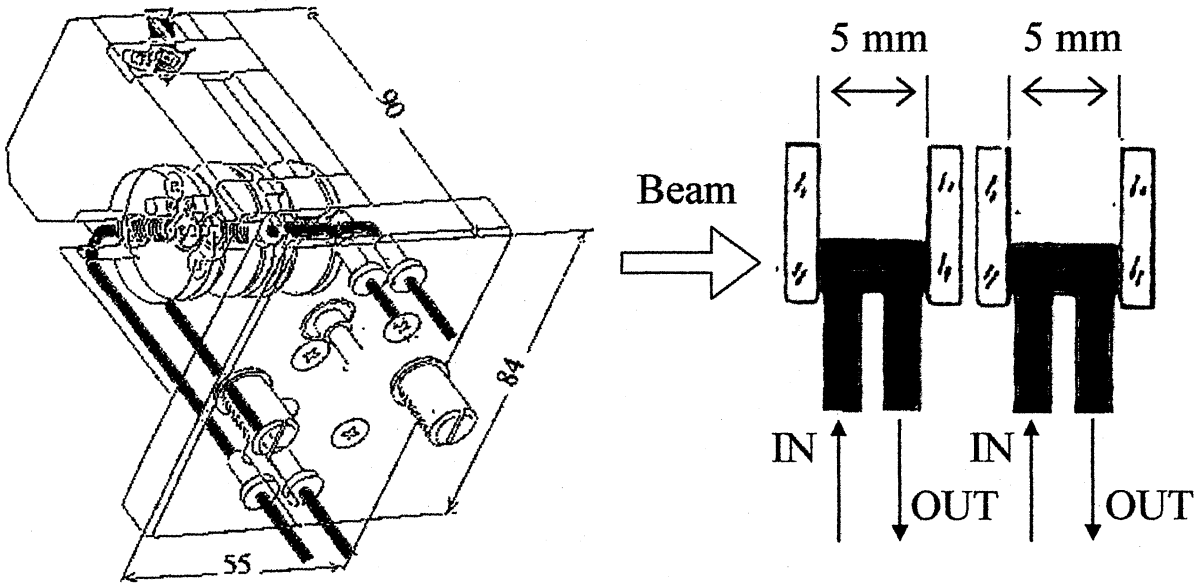

Path length, 5 mm; cell volume, 4 μl.

Fig. 3-2 Configuration of a serial flow cell and single beam detection system

3.2.3. Procedure

A carrier solution (C, 0.5 M hydrogen peroxide at pH 2) and a R_1 solution (0.08 M *p*-anisidine, 0.06 M DMA, 0.2 M acetate buffer at pH 3.1 and 2×10^{-3} M diphosphate) were delivered at 0.65 ml min^{-1} by a pump 1 (P_1). The carrier solution (described above) and an R_2 solution (0.06 M *p*-anisidine, 0.06 M DMA, 0.2 M acetate buffer at pH 3.1, 2×10^{-3} M diphosphate and 2×10^{-3} M phen) were delivered at 0.70 ml min^{-1} by a pump 2 (P_2). The sample (S) and 3 M hydrogen peroxide (pH 2, R_3) solutions were delivered by two peristaltic pumps (P_3, P_4). These mixed

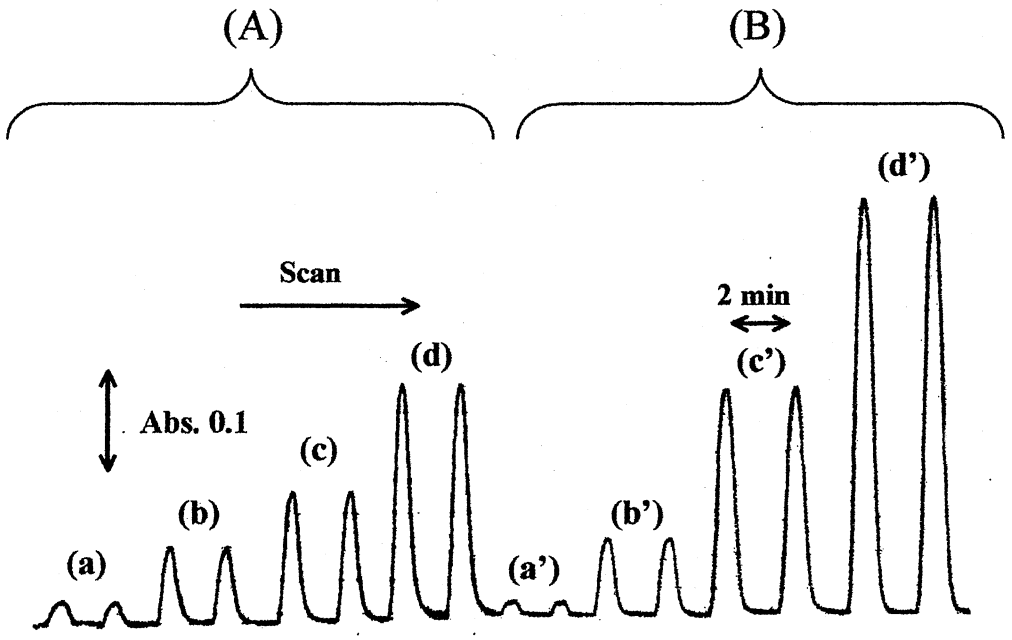

Fig. 3-3 Flow signals for copper(II) and iron(III) using a serial flow cell. (A) peak heights for copper(II), (a) blank (b) 0.5 ppb (c) 1 ppb (d) 2 ppb; (B) peak height for iron(III) (a') blank (b') 20 ppb (c') 50 ppb (d') 100 ppb. Other conditions are the same as in Fig. 3-1.

solutions were loaded in two sample loops (2 m) attached to valves V_1 and V_2, and these solutions were injected into the carrier solutions. The absorbance of the dye formed in the reaction coil (RC) and the cooling coil (CC) was monitored at 740 nm using a double-beam spectrophotometer equipped with the serial flow cell and recorded on a recorder. Fig. 3-3 shows flow signals for copper(II) and iron(III) obtained using the serial flow cell.

3.3. Results and Discussion

3.3.1. Effects of activators on the catalytic reactions

The use of a suitable activator in the catalytic methods can enhance the catalytic effect of specific metal ions, and then the selectivity and sensitivity can be also improved.

The activating effects of several polypyridines, such as phen, neocuproine, BPS, and BCS were investigated. Fig. 3-4 (a) shows the effects of the phen concentration on the copper- and iron-catalyzed reactions in the range from 0 to 1×10^{-2} M. Phen enhanced the catalytic action of iron(III) and acted as the inhibitor for copper(II). The conditional redox potential of the Fe(III)/Fe(II) system increased in the presence of phen; the overall formation constant of the Fe(II)-phen complex ($\log \beta_3 =$ 21.3) is larger than that of the Fe(III)-phen complex ($\log \beta_3 = 14.1$).[42] Therefore, it was obvious that the coexisting phen enhanced the oxidation power of Fe(III). The absorbance of the produced dye in the presence of iron(III) increased up to 2×10^{-3} M phen, and then the absorbance gradually decreased over that concentration. It seems that the activator was

attributable to form ternary complexs of the activator-metal-substrate[40]; phen-iron-*p*-anisidine and/or phen-iron-DMA. Similarly, the effect of BPS was also studied on the iron-catalyzed dye-formation reaction. However, the absorbance in the presence of BPS was lower than that of phen, because BPS might cause a steric hindrance on the ternary complex formation. Thus, a 2×10^{-3} M phen concentration was selected in the iron(III) determination system.

The effect of neocuproine concentration was investigated on each metal determination system. Neocuproine did not act as the effective activator for copper(II) and iron(III) in the range from 0 to 1×10^{-2} M. This result is shown in Fig. 3-4 (b). Although neocuproine acted as the activator for the

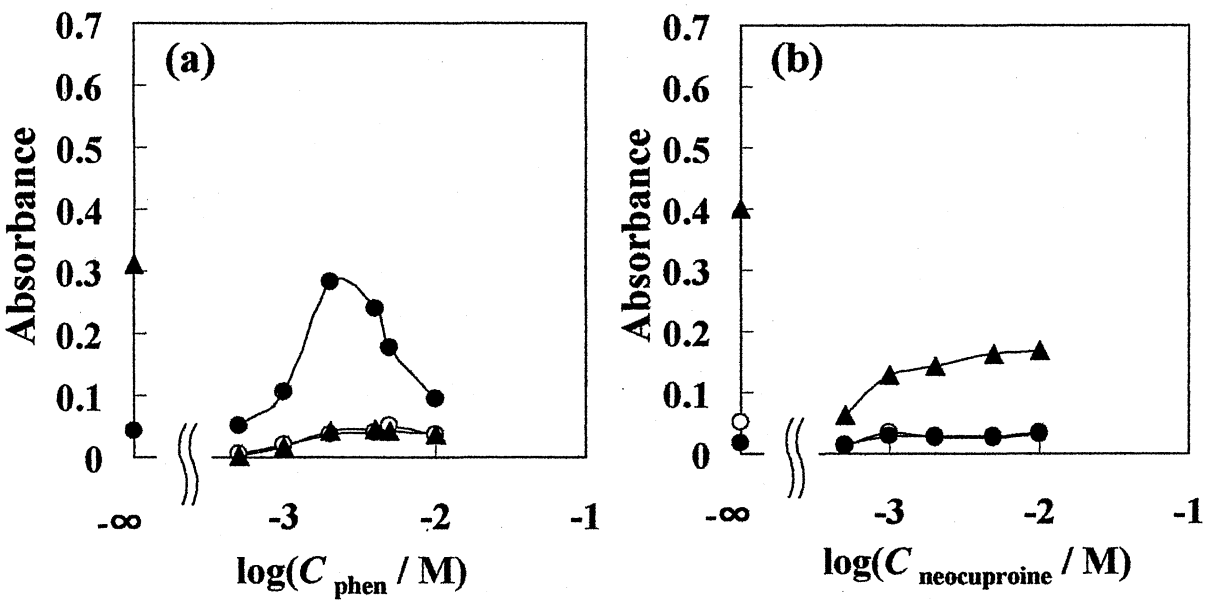

Fig. 3-4 Effects of (a) phen and (b) neocuproine concentration on the copper and iron determination. (▲), 5 ppb copper(II); (△), blank for copper(II); (●), 50 ppb iron(III); (○), blank for iron(III). Other conditions are the same as in Fig. 3-1.

copper-catalyzed reaction,[20] the same result could not be observed in this study. Neocuproine acted as the activator for the copper-catalyzed reaction when the DMA concentration was 0.02 - 0.03 M and the *p*-anisidine concentration was 0.01 M. On the other hand, neocuproine acted as the inhibitor for copper(II) if the concentration of *p*-anisidine was more than 0.02 M. Thus, the activator for copper(II) determination was not used in the present FIA study.

3.3.2. Effect of diphosphate on the determination of copper(II) and iron(III)

In the previous study[20], diphosphate was effective as the masking agent to determine copper(II) and iron(III) successively. The effects of diphosphate for copper(II) and iron(III) were investigated in the proposed FIA system. The recoveries are given in Table 3-1. The recoveries in the absence of diphosphate were over 100%. This is because copper(II) and iron(III) catalyze in the same indicator reaction. In the presence of diphosphate, the recoveries of copper(II) and iron(III) were around 100%, because all catalytic actions were slightly inhibited.

Table 3-1 Recoveries of copper(II) and iron(III) with and without diphosphate

Added/ppb		Found/ppb			
		Cu		Fe	
Cu	Fe	With	Without	With	Without
5	50	5.16 (103)*	6.01 (120)*	51.3 (103)*	63.7 (127)*
1	20	0.99 (99)*	1.06 (106)*	20.1 (101)*	28.8 (144)*
1	50	1.04 (104)*	1.11 (111)*	49.5 (99)*	65.2 (130)*

* Recovery, %

The effect of the diphosphate concentration on the copper- and iron-catalyzed dye formation was investigated. The results are shown in Fig. 3-5. The interferences for each element were restricted with increasing the diphosphate concentration. It seems that the complex formation of these metals with diphosphate occurred. In addition, the peak heights of the reagent blank were depressed in the presence of diphosphate. Thus, a 2×10^{-3} M diphosphate solution was selected on each determination of copper(II) and iron(III).

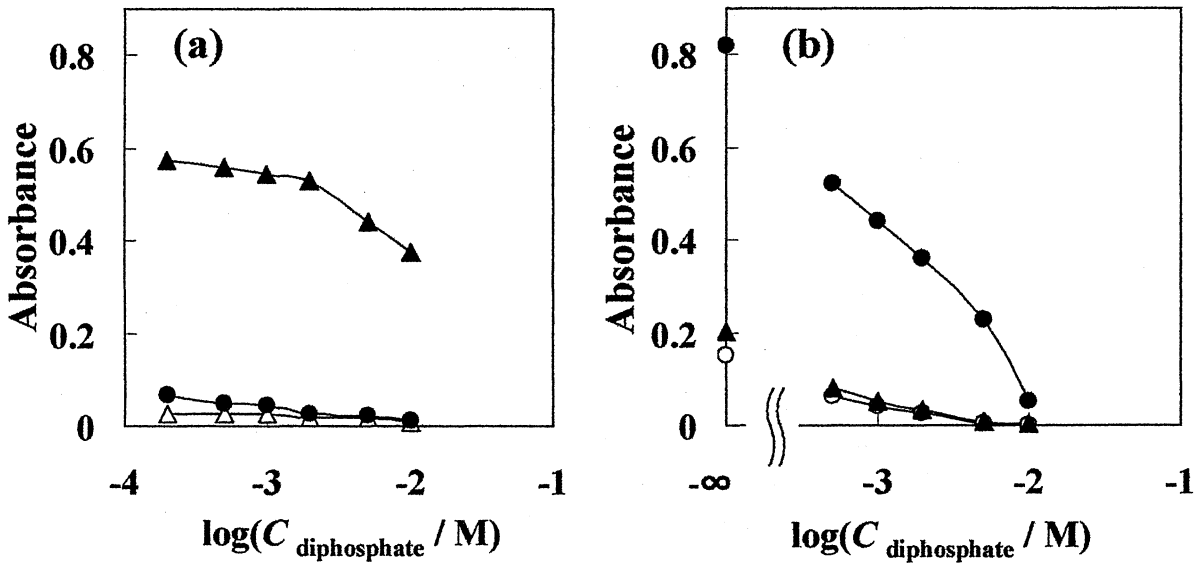

Fig. 3-5 Effects of diphosphate concentration on the (a) copper and (b) iron determination. (▲), 5 ppb copper(II); (△), blank for copper(II); (●), 50 ppb iron(III); (○), blank for iron(III). Other conditions are the same as in Fig. 3-1.

3.3.3. Optimization of the hydrogen peroxide concentration

The hydrogen peroxide concentration in samples was varied from 0 to 4 M. The absorbance of the dye increased with increasing the hydrogen peroxide concentration. Therefore, a 3 M hydrogen peroxide solution was selected on the determinations of copper(II) and iron(III). However, the peak heights of the reagent blank became high with an increase in the concentration of hydrogen peroxide. Consequently, hydrogen peroxide was added to each carrier solution (pH 2) to reduce blank peak heights. The concentration was varied from 0 to 1 M. The results are shown in Figs. 3-6 (a) and (b). All blank peak heights were reduced with increasing the concentration in the carriers. Thus, the hydrogen peroxide concentrations in the carriers and sample solution were selected to be as 0.5 and 3 M, respectively.

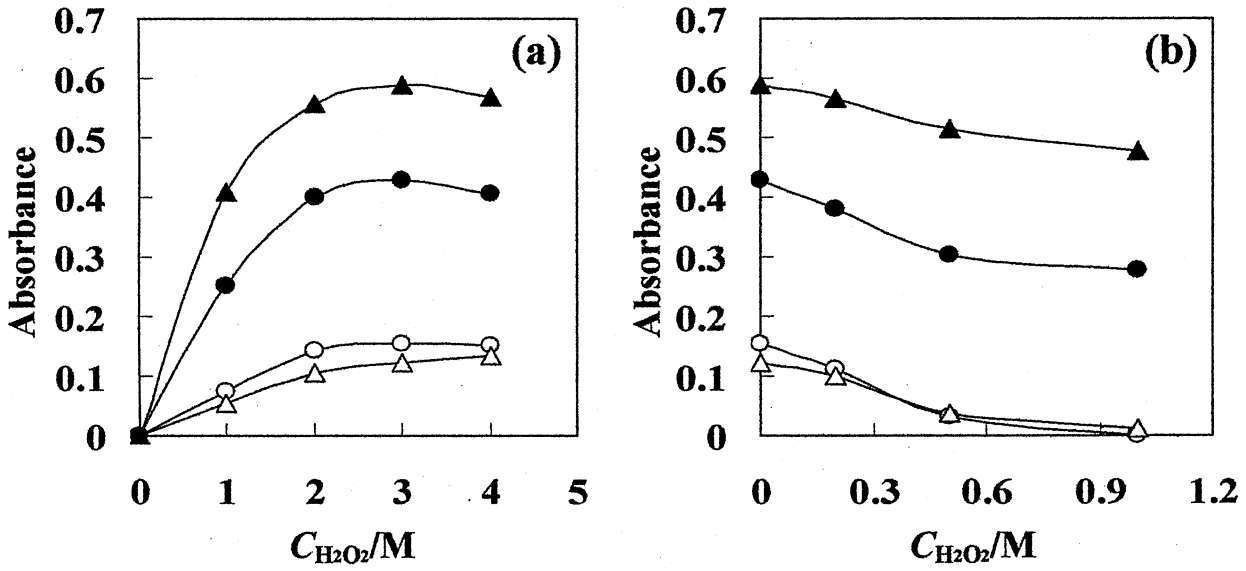

Fig. 3-6 Effects of hydrogen peroxide concentration (a) in sample and (b) in carrier. (▲), 5 ppb copper(II); (△), blank for copper(II) determination. (●), 50 ppb iron(III); (○), blank for iron(III) determination system. Other conditions are the same as in Fig. 3-1.

3.3.4. *Optimization of pH*

The effects of pH were investigated over the range of 2.1 - 3.5 for copper(II) and 2.3 - 3.4 for iron(III). The results are shown in Fig. 3-7. pH was measured after merging in the tube. In both catalysts, the highest peak was obtained at around pH 2.8. Therefore, the reaction pH was fixed at pH 2.8.

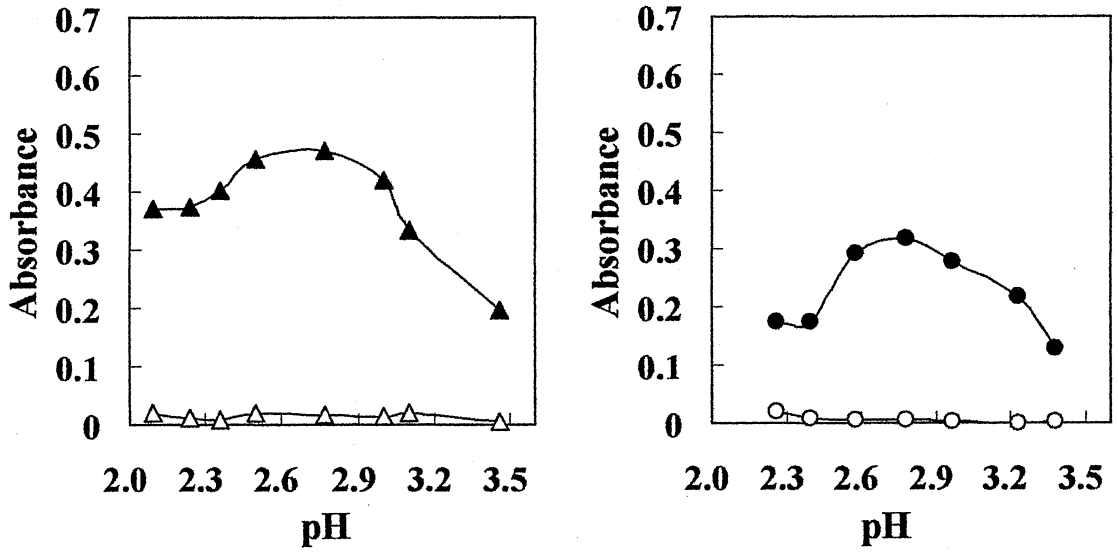

Fig. 3-7 Effects of pH on the dye-formation.. (▲), 5 ppb copper(II); (△), blank for copper(II) determination; (●), 50 ppb iron(III); (○), blank for iron(III) determination system. Other conditions are the same as in Fig. 3-1.

3.3.5. *Optimization of the reaction temperature*

The effects of the reaction temperature on the dye formation in the absence and/or presence of copper(II) and iron(III) were studied in the range from 24 to 95℃. The results are shown in Fig. 3-8. The peak heights increased with an increase in the temperature in the presence of catalysts.

On the other hand, the peak heights in the absence of catalysts were low. Thus, the reaction temperature was set to be 90℃.

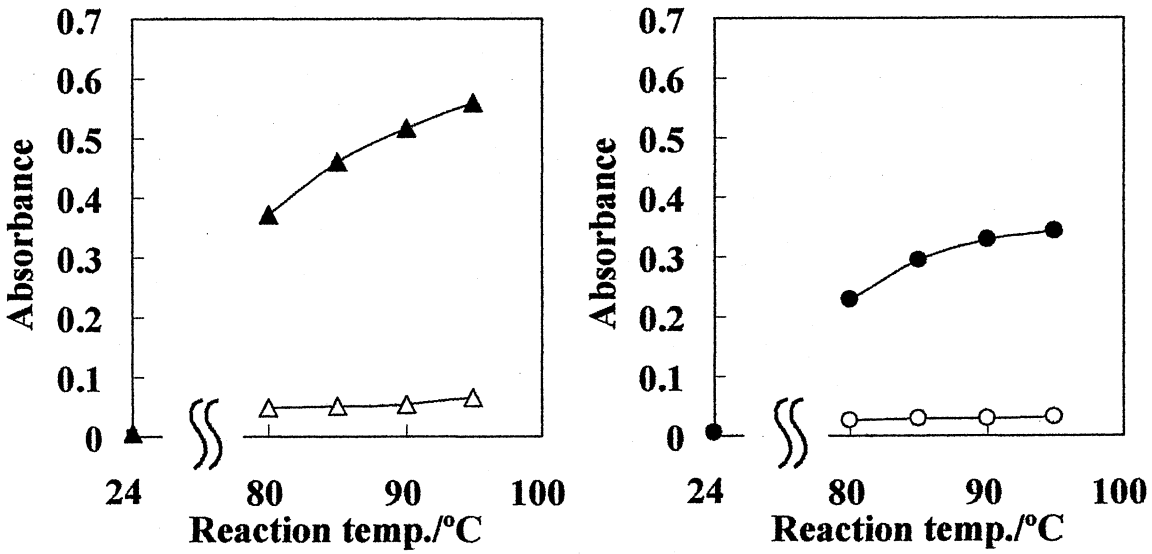

Fig. 3-8 Effects of reaction temperature on the dye-formation. (▲), 5 ppb copper(II); (△), blank for copper(II) determination; (●), 50 ppb iron(III); (○), blank for iron(III) determination. Other conditions are the same as in Fig. 3-1.

3.3.6. Optimization of other variables

The effects of other reagent concentrations were examined. The *p*-anisidine concentration was varied from 0 to 0.1 M. The absorbance increased with increasing its concentration. The 0.1 M and 0.08 M *p*-anisidine concentrations were selected for the copper(II) and iron(III) detection, respectively. The DMA concentration was varied from 0 to 0.08 M. In this study, 0.06 M DMA was used. The reaction coil length was varied from 2 to 10 m on the copper-(or iron-) catalyzed dye-forming

reaction. When the length became longer than 6 m for copper(II) and 8 m for iron(III), the absorbance of the dye increased. Thus, a reaction coil length of 8 m was selected for the determination of copper(II) and iron(III).

The slower flow rate resulted in an increase of the absorbance because the reaction time was longer. Flow rates of 1.3 and 1.4 ml min^{-1} were used for the copper(II) and iron(III) detection. The sample loops (0.5 mm i.d.) for the copper- and iron-assay system were varied from 0.5 to 3 m. Taking into account the sensitivity and repeatability, sample loops of 2 m were selected.

3.3.7. Calibration curves for copper(II) and iron(III)

The calibration curves for copper(II) and iron(III) were prepared under the optimum conditions(Table 3-2). The calibration curves are shown in Fig. 3-9. The dynamic ranges were 0.05 - 5 ppb for copper(II) and 0.5 - 100 ppb for iron(III), respectively. The sampling rate was 30 sample h^{-1} for each analysis. The RSD (n = 10) by the FIA system were 0.96% and 0.46% for 0.5 and 2 ppb copper(II), 0.78% and 0.45% for 20 and 50 ppb iron(III), respectively. The detection limits (3σ) were 10 ppt for copper(II) and 100 ppt for iron(III) and the detection system gave the excellent sensitivity in FIA spectroscopy.

Successive determinations of copper(II) and iron(III) in artificial mixtures were studied. The results are given in Table 3-3. An error of ±5% was considered to be tolerable. The concentration ranges were 0.5 - 2 ppb for copper and 10 - 200 ppb for iron. The 100 ppb iron(III) showed no interference in the determination of 0.5 ppb copper(II). And also, 10 ppb iron(III) did not interfere in the determination of 1 ppb copper(II).

Table 3-2 Experimental conditions by the proposed FIA method

Cu	Fe
0.08 M *p*-Anisidine	0.06 M *p*-Anisidine
0.06 M DMA	0.06 M DMA
0.2 M Acetate buffer (pH 3.1)	0.2 M Acetate buffer (pH 3.1)
2×10^{-3} M Diphosphate	2×10^{-3} M Diphosphate
	2×10^{-3} M phen
0.5 M H_2O_2 at pH 2 (carrier)	0.5 M H_2O_2 at pH 2 (carrier)
3 M H_2O_2 at pH 2 (inject)	3 M H_2O_2 at pH 2 (inject)
RC 8 m, 90°C, ϕ 0.5 mm	RC 8 m, 90°C, ϕ 0.5 mm
CC 1 m, ϕ 0.5 mm	CC 1 m, ϕ 0.5 mm
SL 2 m, ϕ 0.5 mm	SL 2 m, ϕ 0.5 mm
BPC 35 cm, ϕ 0.25 mm	BPC 35 cm, ϕ 0.25 mm
Flow rate, 1.4 ml min^{-1}	Flow rate, 1.3 ml min^{-1}
λ_{max}, 740 nm	λ_{max}, 740 nm

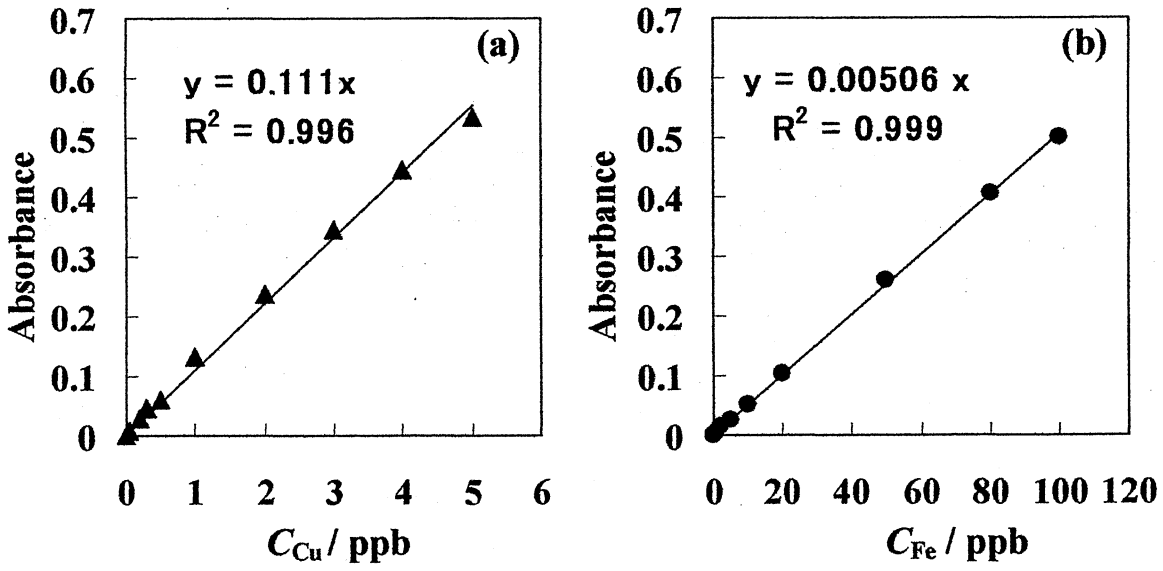

Fig. 3-9 Calibration curves for copper (a) and iron (b) under the optimum condtions. Other conditions are the same as in Fig. 3-1.

Table 3-3 Recovery tests of copper(II) and iron(III) in synthesized solutions

Added / ppb		Found / ppb		Recovery / %	
Cu	Fe	Cu	Fe	Cu	Fe
0.5	20	0.51	19.6	101	98
0.5	50	0.52	52.0	104	104
0.5	100	0.50	95.7	100	96
1	10	0.99	9.76	99	98
1	100	0.96	99	96	99
1	200	1.05	-	105	-
2	100	2.10	99	105	99
2	200	2.09	-	105	-

3.3.8. Interferences of foreign ions in the determination of copper(II) and iron(III)

The interferences of foreign ions in the determination of a mixture of 2 ppb copper(II) and 50 ppb iron(III) were examined. The results are summarized in Table 3-4, where the tolerable concentrations of foreign ions are shown in each case. An error of ±5% was considered to be tolerable. Most of the metal ions and inorganic anions did not interfere in the determinations of copper(II) and iron(III) for concentrations of up to at least 200 ppb.

Table 3-4 Interferences of foreign ions in the successive determination of 2 ppb copper(II) and 50 ppb iron(III)

Added[a] / ppb	Cu	Fe
50000	K(I), Mg(II), SO_4^{2-}, Cl^-, NO_3^-	K(I), Na(I), SO_4^{2-}, Cl^-, NO_3^-
20000	Na(I), Ca(II)	
10000	BO_3^{3-}, Cd(II)	Cd(II), BO_3^{3-}, Mg(II), Ca(II)
5000		Zn(II)
1000	Co(II)	Mn(II), Co(II)
500	Mn(II), Zn(II), Al(III)	Pb(II)
200	Pb(II), Cr(VI), Ni(II)	Cr(VI), Al(III), Ni(II)

a. Tolerable concentration with the tolerance range 95 - 105%, which means within 5% error in analysis.

3.3.9. Application to standard river water samples and real samples

The proposed method with a newly designed serial flow cell was applied to the successive determination of copper(II) and iron(III) in standard river water samples(JAC 0031 and 0032) issued from Japan Society for Analytical Chemistry. These samples were diluted 5 times with water. Since the pH of the diluted river water was 1.9, the diluted sample did not give any pH effect for copper and iron detection in the FI system. The results are given in Table 3-5. Copper and iron obtained by the proposed method were in good agreement with the certified values.

To examine the applicability of the proposed method, copper(II) (0 - 0.5 ppb) and iron(III) (0 – 5 ppb) standard solutions were added to tap, rain, and well water samples. These real samples were acidified by adding conc. hydrochloric acid to pH ca. 2 after filtering through a Millipore membrane filter (0.45 μm pore size). The results were given in Table 3-6. In these

experiments, good precisions on the determination of copper(II) and iron(III) in sample were obtained, ranging from 94 to 104% (mean 99%).

Table 3-5 Simultaneous determination of copper and iron in standard river water[a]

Sample	Found[b] / ppb		Certified values / ppb	
	Cu	Fe	Cu	Fe
JAC 0031	0.91± 0.03[c]	7.5±0.2[c]	0.88± 0.3	6.9±0.5
JAC 0032	10.4 ± 0.1[c]	56 ±1[c]	10.5 ± 0.2	57 ±2

a. Purchased from Japan Society for Analytical Chemistry.
b. Average value for 10 determinations.
c. The river water was diluted 5 times.

Table 3-6 Determination of copper and iron in tap and natural water samples

Sample	Dilution[a.]		In sample/ppb	
	Cu	Fe	Cu	Fe
Tap	5	5	1.36±0.06	63.4 ±0.6
Rain	1.25	1.25	0.35±0.00	1.78±0.02
Well 1	20	20	5.05±0.19	82.4 ±0.8
Well 2	50	50	73.8 ±0.5	43.0 ±3.4

a. The sample was diluted before injection in the carrier stream

3.3.10. Measurement of labile and inert complexes at pH 5.6 and 1

Artificial samples containing humic acid and copper(II) (or iron(III)) were prepared. The copper(II) concentration was 4 ppb and that of iron(III)

was 100 ppb. Then, the labile and inert complexes at pH 5.6 and 1 were analyzed using the proposed method. The results are given in Table 3-7. The recoveries of copper(II) and iron(III) at pH 5.6 were smaller than their added amounts. The results indicate that copper(II) and iron(III) may form inert complexes with humic acid. However, the recovered amounts of copper(II) and iron(III) at pH 1 were larger than those at pH 5.6. The result suggests that the humic acid complexes with metals dissociate in the lower pH media and labile ions increase in the solution.

Table 3-7 Measurements of labile and inert complexes at pH 5.6 and 1 in artificial samples containing humic acid with copper(II) or iron(III)

Added / ppb		Cu found / ppb		Fe found / ppb	
Cu : Hu[a]	Fe : Hu[a]	pH 5.6	pH 1	pH 5.6	pH 1
4 : 100	100 : 500	2.5±0.0	3.5±0.1	47.1±0.8	89.5±1.0
4 : 200	100 : 1000	1.9±0.0	3.2±0.0	24.8±1.1	85.2±0.4

a. Humic acid.

3. 4. Conclusion

Trace amounts of copper(II) and iron(III) could be successively determined by the proposed FIA system equipped with a newly designed serial flow cell, based on their catalytic effects. The proposed FIA system has wider determinable ranges of 0.05 – 5 ppb copper(II) and 0.5 – 100 ppb iron(III), respectively. This method was successfully applied to the determination of copper(II) and iron(III) in standard river water samples as well as tap, rain, and well water samples without any preconcentration or separation. Also, it was useful to assay labile copper(II) and iron(III) complexes in natural water.

Chapter 4 Effect of nitro-PAPS on the reduction of iron(III) with cobalt(II) and flow-injection determination of cobalt(II) in real samples[56]

4.1. Introduction

A cobalt alloy contains chromium, tungsten, or molybdenum, and it has some advantages such as high hardness and endurance against oxidation.[57] This alloy is used as medical instruments[58], glass frame, scissors, and accessory and so on. And also, it is well-known that cobalt exists in the center of vitamin B_{12} which participates in blood formation in human body. Thus, indirect determination of Vitamin B_{12} can be possible by detecting cobalt.[59] Since the decrease of Vitamin B_{12} in human body may cause neuralgia, pernicious anemia, and eyestrain[60], the vitamin is compounded into supplements and eye lotions. Therefore, highly sensitive analytical method for the determination of cobalt is required for the quality control in various fields.

The standard redox potential of Co(III)/Co(II) system is 1.81 (vs. NHE)[61], and Co(III) rarely exists in aqueous solution. It means that Co(III) obtained by electrolysis can be used as a strong oxidation reagent.[62] Co(II) is easily oxidized to Co(III) in the presence of an appropriate ligand which forms the corresponding stable complex with Co(III). Vydra and Pribil[63,64] reported that the conditional redox potential of $Co(phen)_3^{3+}/Co(phen)_3^{2+}$ at pH 2 was 0.37 V. Teshima et al. developed the novel redox system of Co(II) with V(V), Cr(VI)[65], and Ce(IV)[66] in the presence of 2,2'-bipyridyl or phen and reported a titrimety for the simultaneous determination of Cr(VI) and Fe(III) in high carbon ferrochrome using phen.[67]

Water-soluble pyridylazo compound such as 2-(5-nitro-2-pyridylazo)-5-(*N*-propyl-*N*-sulfopropylamino)phenol (nitro-PAPS)[68] was synthesized as a sensitive chromogenic reagent for the determination of metal ions.

Makino et al.[69,70] and Ohno et al.[71] have reported the sensitive colorimetric determination of heavy metal using nitro-PAPS in serum. Nitro-PAPS was used as pre-column chelating agent in HPLC[72-74] and was also utilized for the determination of iron[75] or vanadium[76] by FIA. However, the effect of ligand on the redox reaction of metal ion has been never discussed quantitatively so far.

In this chapter, the redox reaction of Co(II) with Fe(III) is investigated titrimetically in the presence of nitro-PAPS. As a result, it is proved that Co(II) reduces Fe(III) to Fe(II) in the presence of nitro-PAPS. The rapid and highly sensitive FI system is developed for the determination of Co(II) by measuring the specific absorption of the produced Fe(II)-nitro-PAPS complex. This method is successfully applied to the determination of Co(II) in cobalt alloy, pepperbush, and pharmaceuticals.

4.2. Experimental

4.2.1. Reagents

A 2.5×10^{-3} M nitro-PAPS solution was prepared by dissolving 0.126 g of nitro-PAPS (Dojin) in water and made up to 100 ml with water.

A 2.0×10^{-2} M cobalt(II) solution was prepared by dissolving 2.380 g of cobalt(II) chloride hexahydrate (Wako) in 5×10^{-2} M sulfuric acid and made up to 500 ml. The stock solution was prepared by suitable dilution with 0.01 M hydrochloric acid.

A 2.0×10^{-2} M iron(III) solution was prepared by dissolving 4.822 g of ammonium iron(III) sulfate decahydrate (Wako) in 0.5 M sulfuric acid and made up to 500 ml.

Cobalt(II) and iron(III) were standardized by EDTA titration.

A 1 M acetic acid solution was prepared by diluting 28.6 ml of acetic acid (Sigma Aldrich Japan, Tokyo) to 500 ml with water. A 1 M sodium acetate solution was prepared by dissolving 8.203 g of sodium acetate (Nakalai Tesque, Kyoto) with water and made up to 100 ml with water. These solutions were mixed to prepare a buffer solution at pH 3.5.

4.2.2. Apparatus

A Mitsubishi Chemical Model GT-07 automatic titrator was used for the potential difference measurement. A Horiba Model F-22 pH/mV meter was used for pH adjustment. A V-560 double-beam spectrophotometer was used with 10 mm light-path cells for absorbance measurements.

The system was consists of an intelligent HPLC pump (PU-1580, Jasco co.), a six-way injection valve (FLOM), a spectrophotometer (S-3250, Soma Optics) with a flow cell (cell volume: 8μl) and a FIA monitor (F·I·A co.) for record. The same kind of Teflon tubing described previously was used for the manifold.

4.2.3. Procedure

A carrier solution (CS, 0.01 M hydrochloric acid) and a reagent solution (RS, 0.5 M acetate buffer at pH 3.5, 2×10^{-5} M Fe(III), 2.5×10^{-4} M nitro-PAPS) were delivered at 1.5 ml min^{-1} by the pump 1 (P_1). The sample

(200 μl) was injected into the carrier solution and merged with the R_1 solution. The absorbance of the Fe(II)-nitro-PAPS complex formed in the reaction coil (RC, 3 m length) was monitored at 790 nm using a double-beam spectrophotometer and recorded on a recorder. Fig. 4-1 and Fig. 4-2 show flow system and flow signals for cobalt(II).

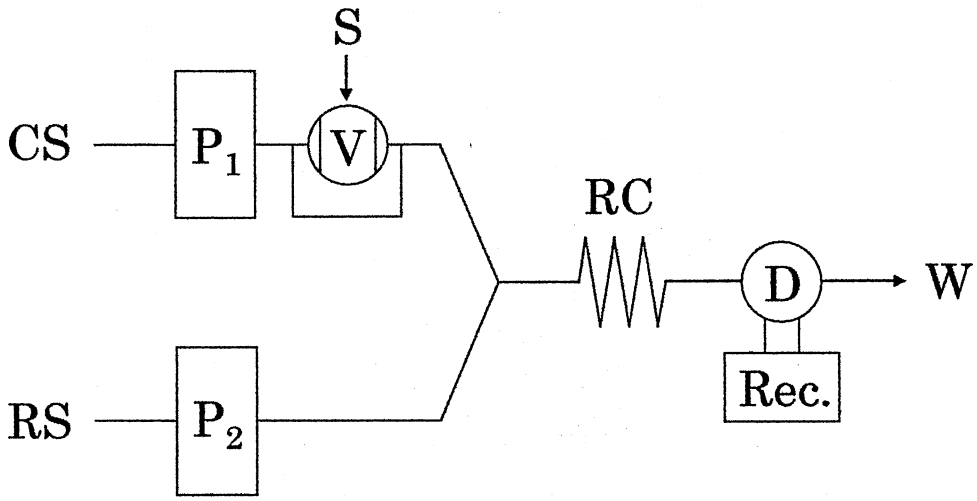

Fig. 4-1 Flow system for the determination of cobalt(II). CS: 0.01 M HCl; RS: a mixed solution of 2.0×10^{-5} M Fe(III), 2.5×10^{-4} M Nitro-PAPS and 0.5 M acetate buffer (pH 3.5); P_1 and P_2: pump (flow rate 1.5 ml/min each pump); RC: reaction coil (3 m×i.d. 0.5 mm); D: spectrophotometer; S: sample (200 μl); V: six-way valve; Rec.: recorder; W: waste.

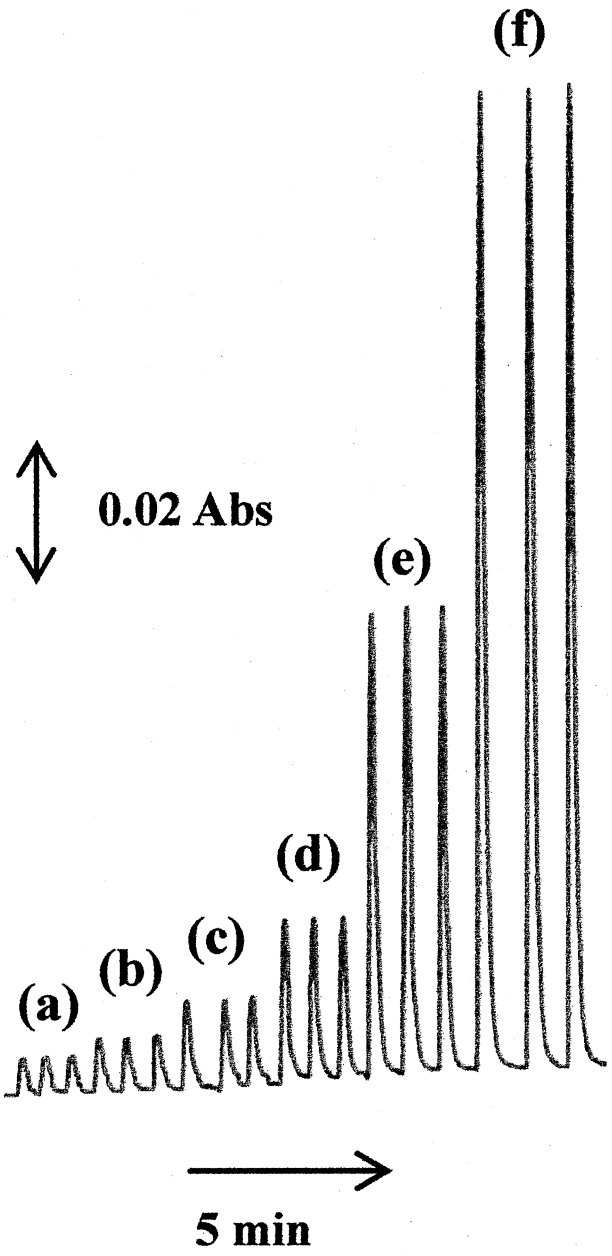

Fig. 4-2 Flow signals for cobalt(II) analysis. (a), 5.0×10^{-7} M; (b), 7.5×10^{-7} M; (c), 1.0×10^{-6} M; (d) 2.0×10^{-6} M; (e) 5.0×10^{-6} M; (f) 1.0×10^{-5} M. Other conditions are the same as in Fig. 4-1.

4.3. Results and Discussion

4.3.1. The reduction of iron(III) with cobalt(II)

The equilibrium constant ($K_{Co\text{-}Fe}$) is calculated to be $10^{-17.6}$ from the standard redox potentials of $E°_{Co}$ (1.81 V vs. NHE) and $E°_{Fe}$ (0.771 V vs. NHE).[61] Thus, this reduction of Fe(III) with Co(II) can not proceed.

$$Co(II) + Fe(III) \underset{}{\overset{K_{Co\text{-}Fe}}{\rightleftharpoons}} Co(III) + Fe(II)$$

If a suitable ligand that can form a stable complex with Co(III) and Fe(II) exists, the equilibrium constant can be improved. The effect of nitro-PAPS on the reduction was studied. The result is shown in Fig. 4-3.

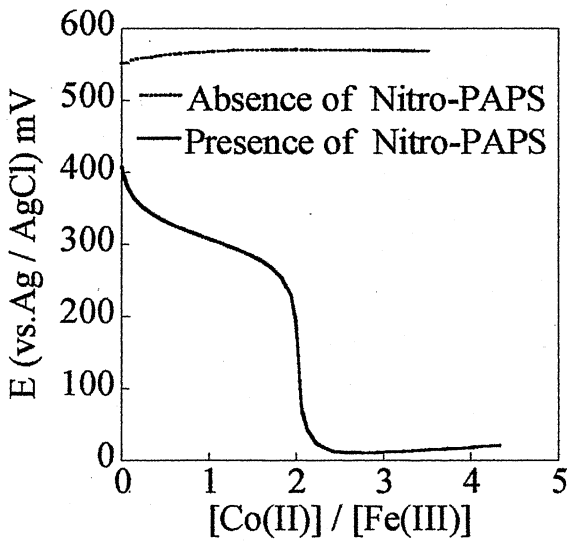

Fig. 4-3 Effect of Nitro-PAPS on the titration of Fe(III) with Co(II). Titrand (20 ml taken): a mixed solution of 5×10^{-4} M iron(III), 1.5×10^{-3} M Nitro-PAPS and 0.25 M acetate buffer (pH 3.5); Titrant: 5×10^{-3} M cobalt(II).

The potential break did not appear in the absence of nitro-PAPS. It means that Co(II) can not reduce Fe(III) to Fe(II). On the other hand, a potential break was obtained in the presence of nitro-PAPS and nitro-PAPS was effective on the redox system. The effect of pH on the titration curve was studied. The end point was detected at the equilibrium point in the range of pH 2.5 - 3.5. The conditional equilibrium constant of this redox system estimated from the conditional redox potential was $10^{4.9}$. Although the conditional equilibrium constant is not enough for the determination of cobalt (or iron) by titrimetry, it was enough to apply to spectrophotomery.

4.3.2. Absorption spectrum of iron-nitro-PAPS complex

Fe(II) reacts with nitro-PAPS to form the colored complex (Scheme 4-1).

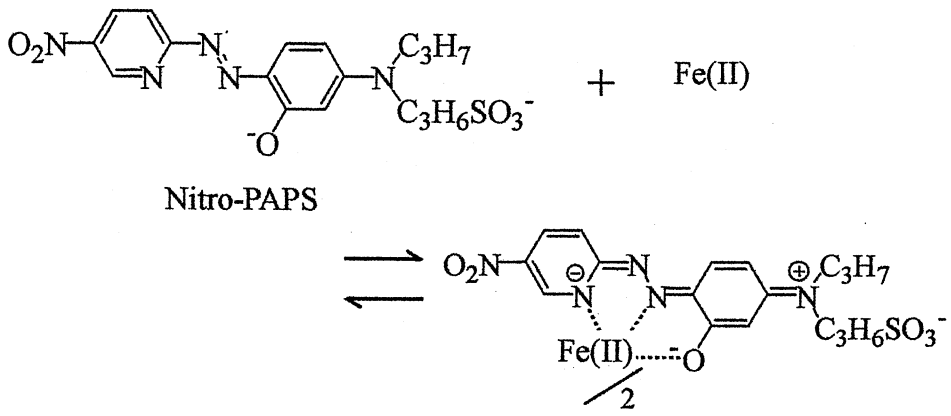

Scheme 4-1

The effect of Co(II) concentration on the Fe(II)-nitro-PAPS complex formation was studied. The result is shown in Fig. 4-4. The absorbance at around 560 nm increased with increasing the molar ratio. When the ratio was over 1, the absorbance increased quantitatively. It means that the

complex formation of Co(II) with nitro-PAPS proceeded at the ratio over 1. Although the absorbance at 790 nm increased with increasing the concentration of Co(II), the absorbance was kept constant at molar ratio over 1. Thus, the absorption at 790 nm was specific on the Fe(II)-nitro-PAPS complex. Although the maximum wavelength of Co(III)-nitro-PAPS complex was at 560 nm, other complexes with copper, zinc, and nickel showed the same color development. Taking into account the selectivity, we selected the monitoring wavelength of 790 nm for the determination of Co(II) in this proposed method.

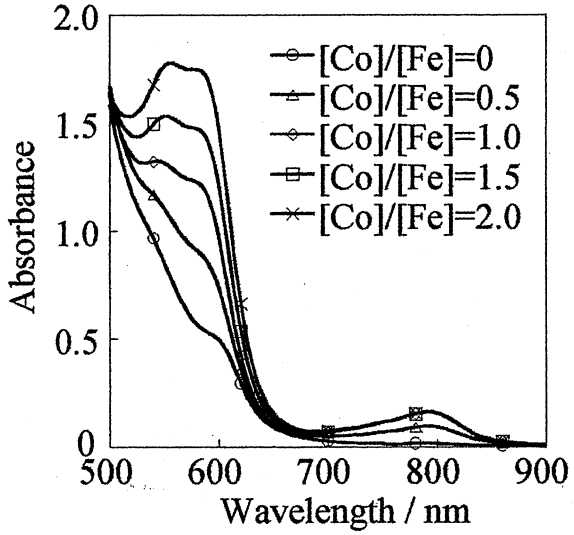

Fig. 4-4 Absorption spectra of iron-nitro-PAPS chelate after reduction with Co(II). [Fe(III)]: 2.5×10^{-6} M; [Nitro-PAPS]: 4×10^{-4} M; [acetate buffer]: 0.25 M (pH 3.5); molar ratio ([Co(II)]/[Fe(III)]): (○) 0 (Fe(III) only); (△) 0.5; (◇) 1.0; (□) 1.5; (×) 2.0.

4.3.3. Optimization of FIA conditions

The effect of pH was investigated over the range of 2.2 - 4.9. The result

is shown in Fig. 4-5. The absorbance increased with increasing pH up to 3.5. pH 3.5 was selected by the result obtained by the potentiometric titration of iron(III) with Co(II) in the presence of nitro-PAPS shown in Fig. 4-3.

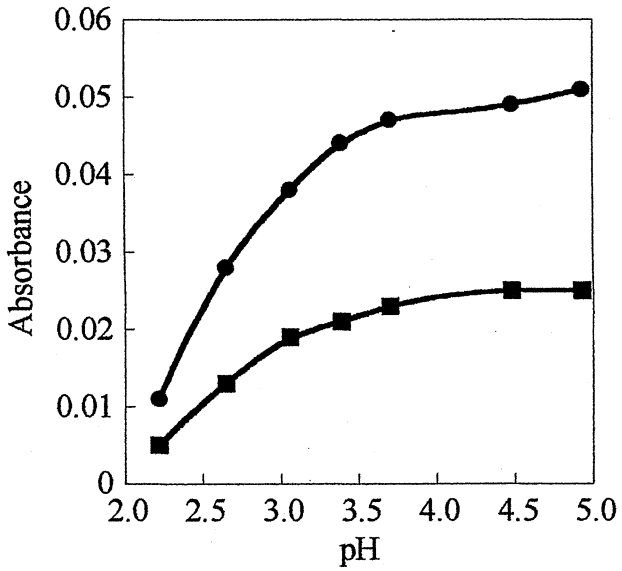

Fig. 4-5 Effect of pH on iron(II)-nitro-PAPS complex. (■) 2.5×10^{-6} M cobalt(II); (●) 5.0×10^{-6} M cobalt(II); other conditions as in Fig. 4-1.

The effect of Fe(III) concentration was varied from 2.5×10^{-6} to 3.0×10^{-6} M. The result is shown in Fig. 4-6. The absorbance was maximum and almost constant over 5×10^{-6} M. Thus, the 2.0×10^{-5} M Fe(III) solution was chosen.

The effect of nitro-PAPS concentration was studied. The peak height was constant more than 2×10^{-4} M. Thus, 2.5×10^{-4} M nitro-PAPS was selected for the determination of Co(II).

The length of RC was varied from 0.5 to 5 m. The peak height was almost constant in the examined RC length. The 3 m RC length was used.

The effect of the flow rate on the peak height was examined in the range 0.5 – 2.0 ml min^{-1}. The peak height of Co(II) was almost constant more

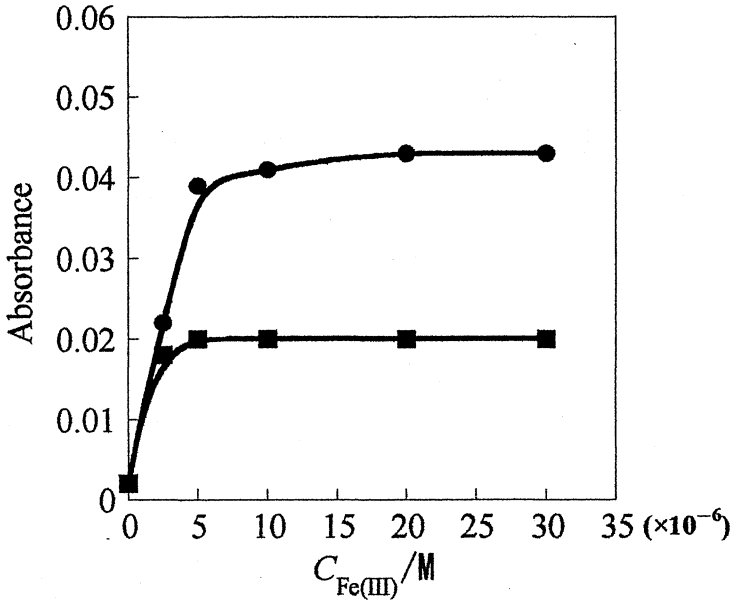

Fig. 4-6 Effect of iron(III) concentration on the peak height of cobalt(II). (■) 2.5×10^{-6} M cobalt(II); (●) 5.0×10^{-6} M cobalt(II); other conditions as in Fig. 4-1.

over 0.75 ml min^{-1}. The flow rate was selected the suitable sampling rate at 1.5 ml min^{-1}.

The sample volume was studied in the range from 120 to 280 μl. The peak height increased with increasing the injected volume. The sample volume was selected to be 200 μl.

4.3.4. Calibration curve for cobalt(II)

The calibration curve for Co(II) was prepared under the optimum condition. The result is given in Fig. 4-7. The dynamic range was 2.5×10^{-7} - 1.0×10^{-5} M for Co(II) ($r^2 = 0.998$). The sampling rate was 70 samples h^{-1}. The relative standard deviation (RSD) (n = 10) was 0.3 % for 2.5×10^{-6} M. The detection limit (3σ) was 1×10^{-7} M for Co(II).

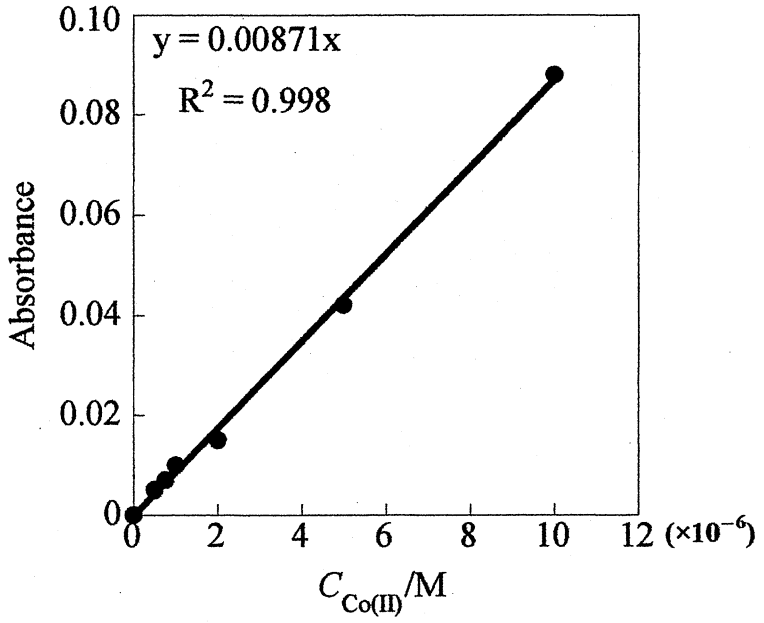

Fig. 4-7 Calibration curve for cobalt(II) in the optimum conditions. Conditions as in Fig. 4-1.

4.3.5. *Effect of interfering ions on the determination of cobalt(II)*

A large amount of iron exists in cobalt alloy and trace amount of iron exist as impurity in eye lotion. Thus, the interference from iron on the determination of cobalt(II) was examined. The maximum absorption wavelength (λ_{max} = 560 nm) of cobalt(III)-nitro-PAPS complex was compared with that (λ_{max} = 790 nm) of iron(II)-nitro-PAPS complex. When the mixed solution of 2.5×10^{-6} M cobalt(II) and iron(III) was injected to the flow system, the peak height measured at 560 nm was 2 times and it means that iron gives big interference. However, the peak height of cobalt(II) at 790 nm was subject to no interference. Thus, the measurement wavelength at 790 nm was chosen.

Table 4-1 summarizes the tolerance limits for foreign ions on the determination of 5×10^{-6} M cobalt(II). An error of ±5 % was considered to

be tolerable. Iron(III), tungsten(VI), nickel(II) and copper(II) showed serious positive interference on the determination of 5×10^{-6} M cobalt(II). However, at the level shown in Table 4-1, these metals do not exist in cobalt alloy and other samples. Accordingly, this proposed method can apply to the determination of cobalt(II) in cobalt alloy. But pepperbush leaves include a large amount of iron. So, it is necessary to remove iron.

Table 4-1 Effect of foreign ions on the determination of 5.0×10^{-6} M cobalt(II)

$\frac{[\text{Ion}]}{[\text{Co(II)}]}$	Added Ion
10000	Na(I), Mg(II), Al(III), K(I), Ca(II) SO_4^{2-}, NO_3^-, CO_3^{2-}
5000	Mn(II)
1000	Cd(II)
200	Zn(II), Rb(I), Sr(II), Ba(II)
50	Si(IV)
20	$Cr_2O_7^{2-}$, Pb(II)
10	VO_2^+, Ni(II), Cu(II)
2	WO_4^{2-}
1	Fe(III)

An error of 5% was considered to be tolerable.

4.3.6. Application to real samples

The proposed method was applied to the determination of cobalt(II) in medicines, cobalt alloy, and pepperbush leaves. The procedure for the decomposition of Vitamin B_{12} (Fig. 4-8), cobalt alloy (Fig. 4-9), and

pepperbush leaves (Fig. 4-10) are described below.

Vitamin B_{12} : Six tablets or 10 ml of eye lotions, 20 ml of conc. hydrochloric acid were taken in a 100 ml beaker. The solution was heated at 200 °C for 2 hours for decomposition. After 10 ml of nitric acid and 2 ml of perchloric acid were added to the beaker, it evaporated to dryness. The residue was dissolved by adding 30 ml of 1 M hydrochloric acid and the solution was diluted to 50 ml with distilled water. The solution was appropriately diluted for the determination.

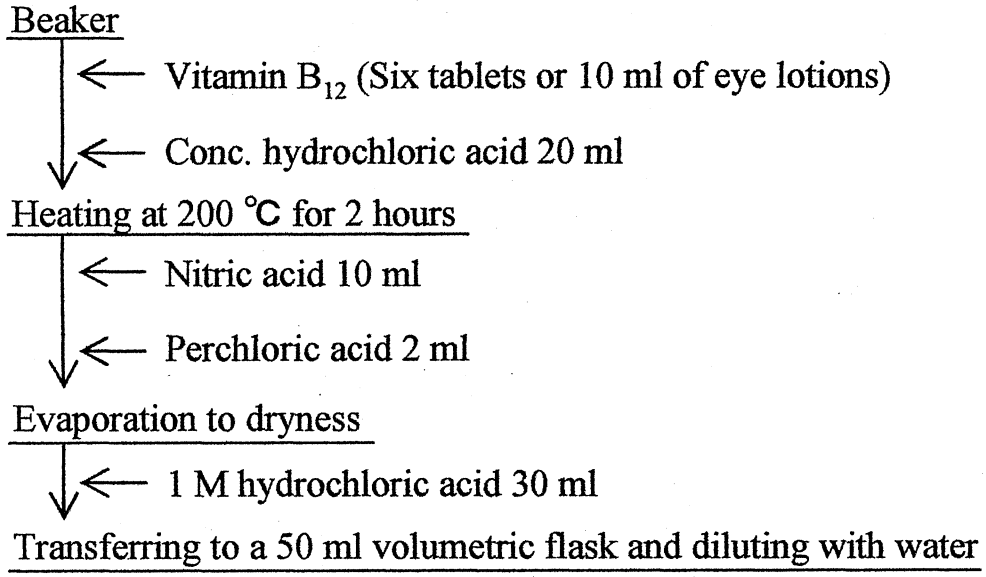

Fig.4-8 Procedure for the decomposition of the Vitamin B_{12} in medicines

Cobalt alloy : The cobalt alloy standard sample (NIST SMR 862; High Temperature Alloy L605) purchased from National Institute of Standard and Technology (NIST) was used. To the vessel, 0.1 g of the sample, 2 ml of conc. nitric acid, 2 ml of conc. hydrochloric acid, and 1 ml of conc. hydrofluoric acid were taken. The mixture was heated at 230 °C for 30

minutes by the microwave digestion labstations (Milestone com.) for the decomposition of cobalt alloy. The solution was diluted to 100 ml with water.

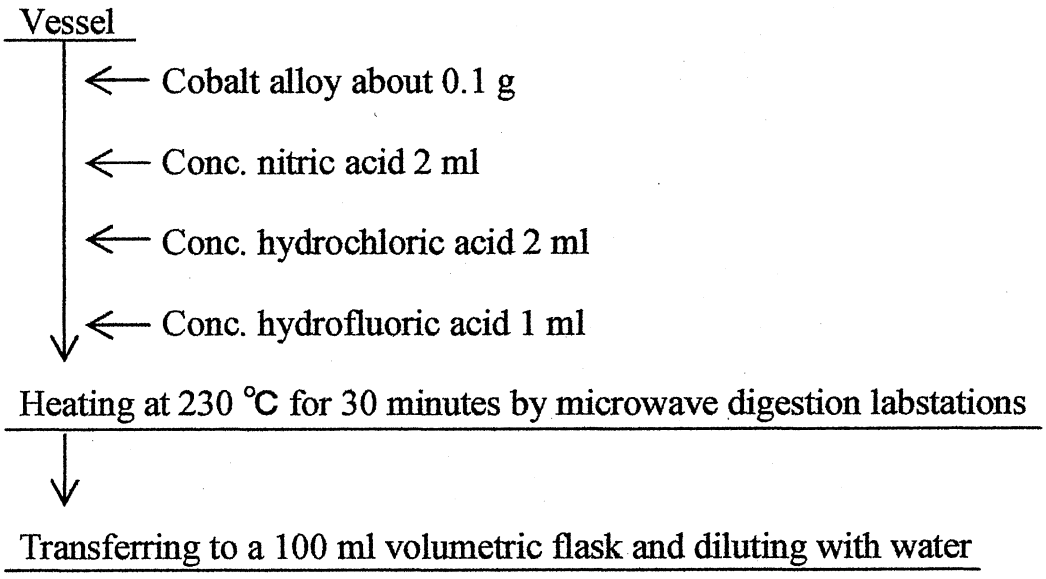

Fig.4-9 Procedure for the decomposition of cobalt alloy

Pepperbush leaves : 0.2 g of pepperbush leaves (NIES No.1) purchased from National Institute for Environmental Studies (NIES) were taken to a small teflon vessel. Two ml of nitric acid, 0.4 ml of perchloric acid and 0.2 ml hydrofluoric acid were added to the vessel. The small vessel was placed in a large teflon vessel in where 1.5 ml of water was put. The large vessel was placed in a stainless vessel, and the solution in the stainless vessel was heated at 90 °C for 2 hours. After that, it was heated at 130 °C for 2 hours, and then it was evaporated to dryness under an infrared lamp on the hot plate. The residue was dissolved by adding 4 ml of 0.1 M hydrochloric acid and was heated to dissolve. To remove iron in the samples, extraction with hinokitiorl/benzene was done. Most of iron was removed by solvent

extraction. The solution was appropriately diluted with 0.01 M hydrochloric acid for the determination.

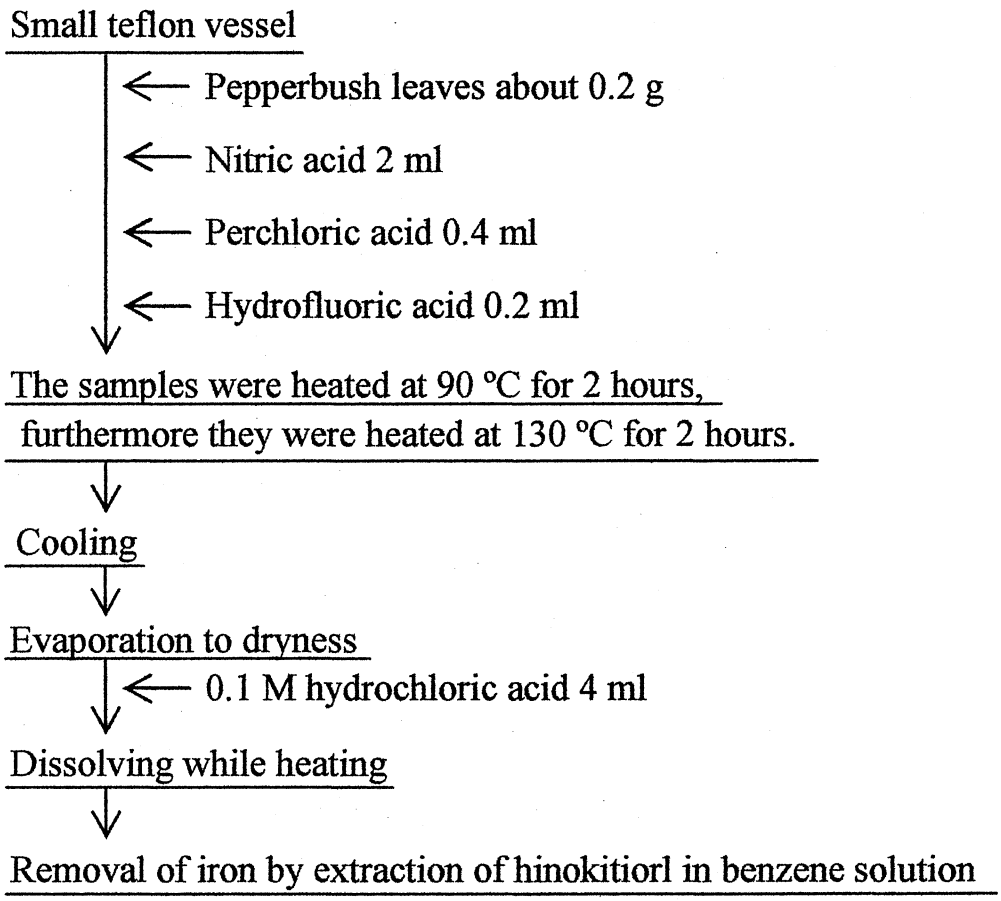

Fig.4-10 Procedure for the decomposition of pepperbush leaves

The analytical results are shown in Table 4-2. The content of Vitamin B_{12} in medicine was estimated from the determination value of cobalt. As a result, these values almost corresponded to the labeled values or certified values.

Table 4-2 Determination of cobalt(II) in practical samples

Sample	Cobalt(II) or Vitamin B_{12} found[a]	Nominal or certified value
Vitamin B_{12}[b]	1430±10 μg / 3 tablets	1500 μg / 3 tablets
Vitamin B_{12}[c]	0.014±0.000$_3$ %	0.015 %
Cobalt alloy	51.1±0.1 %	51.5±0.3 %
Pepperbush leaves[d]	20.7±0.1 μg/g	23±3 μg/g

a. Average for three determinations.

b. Tablet.

c. Eye lotion.

d. The iron in pepperbush leaves was removed by solvent extraction.

4.4. Conclusion

The sensitive and rapid flow-injection spectrophotometric method using the redox reaction of Co(II) with Fe(III) in the presence of nitro-PAPS was investigated. The Fe(II)-nitro-PAPS complex had a specific absorption maximum at 790 nm. Thus, Co(II) could be selectively determined by measuring the absorbance at this wavelength. In the optimum conditions, the calibration curve was linear in the range from 2.5×10^{-7} to 1×10^{-5} M with a sampling throughput of 70 samples h^{-1}. The detection limit (3σ) was 1×10^{-7} M and the RSD for 2.5×10^{-6} M cobalt(II) was within 1%. The proposed method was successfully applied to the analysis of Co(II) in cobalt alloy and pepperbush leaves, and to the indirect determination of Vitamin B_{12} in pharmaceuticals.

Chapter 5 Sequential injection lab-on-valve simultaneous spectrophotometric determination of trace amounts of copper and iron[77]

5. 1. Introduction

Copper and iron are essential elements for living organisms including human being. Lack of these elements in the daily diet may result in the progress of serious diseases. However, excess uptake of copper and iron through water pollution results in acute and/or chronic poisoning. As early as the late 1800s, water pollution occurred as a consequence of industrial waste dumping at the Ashio copper mine in Japan.[78] For sick infants and children, even tap water can cause their chronic copper poisoning.[79] It is well known that sheep are most prone to the copper poisoning.[80] And also, large amount of iron discharged from factories leads to effluvial and reddish water. Recent industrialization in Thailand has exerted considerable stress on the marine environments and provoked habitat degradation.[81] Therefore, the determination of copper and iron is required for quality assessment of wastewater.

The guideline values in wastewater set by Japanese government are 3 mg l^{-1} (mg l^{-1} ≡ ppm) for copper and 10 ppm for iron, respectively.[82] Although spectrophotometric methods with diethyldithiocarbamate and 1,10-phenanthroline are utilized for individual determination of copper and iron,[83] inductively coupled plasma atomic emission spectrometry (ICP-AES) is usually exploited for simultaneous determination of multi-elements including copper and iron. However, the running cost and operator skill requirement for ICP-AES are high, so a cost-effective and affordable technique for copper and iron determination is desired.

Flow injection analysis (FIA) conceived by Ruzicka and Hansen in 1975[6] is one of flow-based techniques and has been applied to many fields such as atmospheric gas analysis,[84] water analysis,[85] bioassay,[86,87] pharmaceutical analysis,[88-90] and so on for the last few decades. Recently, Sakai and co-workers[91] reported a simultaneous spcetrophotometric determination for copper and iron in sera using 2-(5-bromo-2-pyridylazo) -5-[*N*-*n*-propyl-*N*-(3-sulfopropyl)amino]aniline[92] (5-Br-PSAA) by FIA equipped with twin flow cell. The limits of detection (LOD) were 0.39 μg l^{-1} (μg l^{-1} ≡ ppb) for copper and 0.20 ppb for iron. This high sensitivity allowed the volume of serum sample to be minimized. However, analysis of wastewater for copper and iron does not need such highly sensitive method because relatively large volumes of wastewater samples are usually available compared to biological materials. In addition, due to its continuous flow character, FIA essentially tends to consume reagent(s) even when an analyte is not measured.

Sequential injection analysis (SIA) was developed as the second generation of flow injection techniques in 1990.[13,19] In a SIA system, μl volumes of sample and reagents are aspirated at programmed time intervals by a syringe pump that provides for bi-directional discontinuous flow. Therefore, the consumption of reagents and sample in SIA is usually smaller than that in FIA. Moreover, the same SIA setup can be used for different assay protocols without changing configuration of the system. As highlighted in a review by Lenehan et al.,[93] over 200 papers on SIA have been published in the recent decade.

Many researchers utilized sequential injection (SI) technique with UV-VIS detection for the assay of copper[14,94] or iron[15,95-101]. The SI technique was employed as a means of the sample introduction into flame

atomic absorption spectrometric detector for the determination of zinc, manganese, iron, and copper in wine.[17] FI and SI systems with anodic stripping voltammetric detection were exploited for the simultaneous determination of cadmium, copper, lead, and zinc in wastewater samples.[102] SI method with UV-VIS detection has also been utilized for the determination of binary species in water sample: iron(III)-iron(II) using Tiron,[15] chromium(VI)-chromium(III) using 1,5-diphenylcarbazide with wetting film extraction technique,[18] and cobalt(II)-nickel(II) with differential kinetics.[16] However, there is no report on the simultaneous determination of copper and iron by SI system with UV-VIS detection.

Most recently, a mini-conduit module with integrated flow cell and fiber optics was mounted atop a multi-port valve in SI manifold to form a 'lab-on-valve' (LOV).[19] In the SI-LOV system, the volume of the sample path from injector to detector can be minimized. The volume of the generated waste solution is smaller than in a common SI system. This SI-LOV technique was applied to the spectrophotometry for chloride.[103]

This paper describes a SI-LOV system using 5-Br-PSAA as a chromogenic reagent for the simultaneous determination of copper and iron.

The high reagent blank caused by colored 5-Br-PSAA can be successfully suppressed by using spacers including 5-Br-PSAA. The proposed method is useful to determine copper and iron in industrial waste water.

5.2. Experimental

5.2.1. Reagents

Standard copper(II) and iron(III) solution was prepared in the same manner shown in Chapter 2.

A 2×10^{-3} M 5-Br-PSAA stock solution was prepared by dissolving 0.096 g of 2-(5-bromo-2-pyridylazo)-5-[*N*-*n*-propyl-*N*-(3-sulfopropyl)-amino]aniline, sodium salt (Dojindo Laboratories, Kumamoto) in 100 ml of water. 4×10^{-4} (for copper determination) and 7×10^{-4} M (for iron determination) 5-Br-PSAA solutions were prepared by dilution of the stock 5-Br-PSAA solution with water, and a 5×10^{-5} M 5-Br-PSAA solution as a carrier and a spacer as well was prepared by diluting the same stock solution with 0.01 M hydrochloric acid.

A 1×10^{-2} M ascorbic acid solution was daily prepared by dissolving 0.035 g of L-ascorbic acid (Wako) in 10 ml of water. A 5×10^{-4} M L-ascorbic acid solution was prepared by dilution of the stock solution with water.

A 0.2 M acetic acid solution was prepared by diluting 0.6 ml of acetic acid (Sigma Aldrich Japan, Tokyo) to 50 ml with water. A 0.2 M sodium acetate solution was prepared by dissolving 1.35 g of sodium acetate trihydrate (Nakalai Tesque, Kyoto) in 50 ml of water. These solutions were mixed to prepare a buffer solution (pH 4.6).

5.2.2. Apparatus

The scheme of manifold of the computer-controlled SI-LOV system (FIAlab 3000, FIAlab Instruments, USA) used is shown in Fig. 5-1. The system consists of a 2.5 ml syringe pump, a six-port selector valve with integrated flow cell and a single speed unidirectional peristaltic pump. A

UV-VIS spectrophotometer (USB2000, Ocean Optics, USA) was used to measure absorbance of the formed complexes at 558 and 580 nm. A temperature control unit, TC (R-5000C, Sanuki Kogyo, Tokyo) was used to promote the complex formation of iron(II) with 5-Br-PSAA. All flow lines were made from Teflon tubing (0.5 mm or 1 mm i.d., see Fig. 5-1). FIAlab for Windows 2000 software was used to control the SIA-LOV system and to process the experimental data.

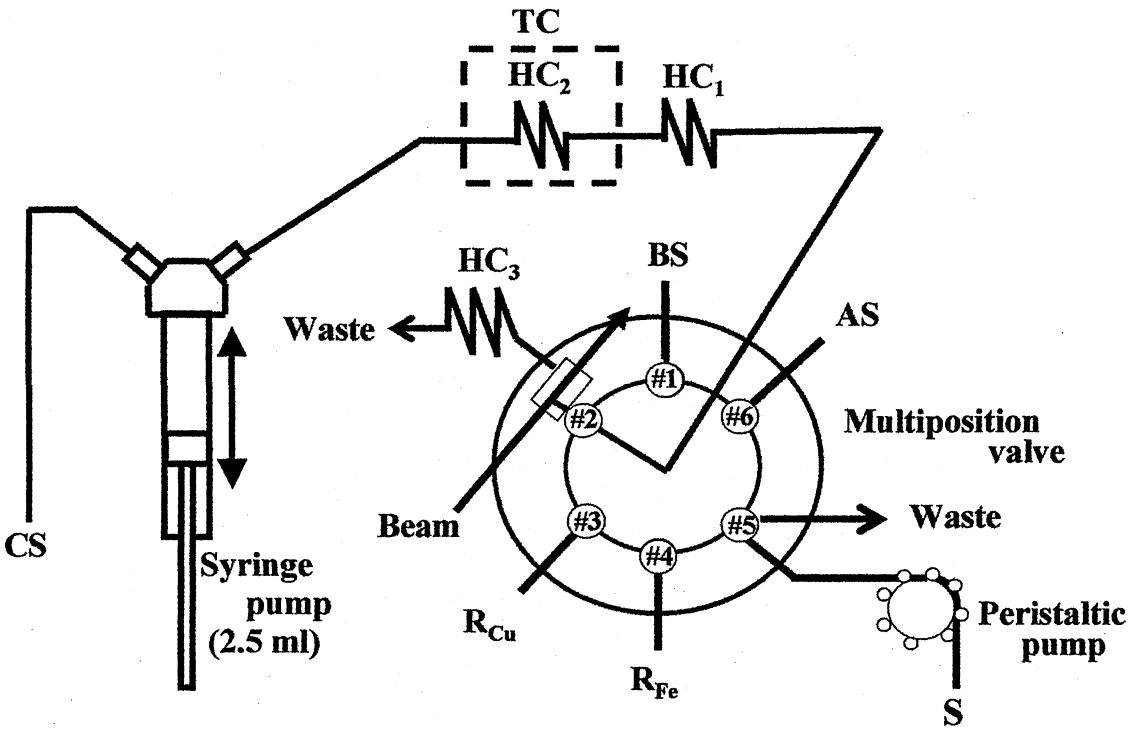

Fig. 5-1 Manifold of the SIA system in the proposed method. HC_1, holding $coil_1$ (0.5 mm i.d., 60 cm); HC_2, holding $coil_2$ (0.5 mm i.d., 55 cm); HC_3, holding $coil_3$ (1 mm i.d., 50 cm); TC, temperature controller (45°C); CS, 5×10^{-5} M 5-Br-PSAA in 0.01 M HCl; R_{Cu}, 4×10^{-4} M 5-Br-PSAA; R_{Fe}, 7×10^{-4} M 5-Br-PSAA; S, sample containing copper and/or iron; AS, 5×10^{-4} M ascorbic acid; BS, 0.2 M acetate buffer at pH 4.6.

A Horiba Model F-22 pH/mV meter equipped with silver/silver chloride electrode (6378-10D, Horiba, Kyoto) was used for pH adjustment.

Phthalate, phosphate and tetraborate pH standard solutions were used for calibration.

5.2.3. Procedure

The central inlet of the six-port valve shown in Fig. 5-1 was connected to a couple of holding coils, HC_1 (0.5 mm i.d., 60 cm) for copper and HC_2 (0.5 mm i.d., 55 cm) for iron. The HC_2 was heated by the above-mentioned TC at 45°C. The flow cell (5 mm path length) was set to the port #2. The auxiliary peristaltic pump was used to transport sample solutions (S) to the sampling line. The sample and reagents were aspirated with a high precision syringe pump of the FIAlab 3000 system. A 0.2 M acetate buffer solution at pH 4.6 (BS), 4×10^{-4} M 5-Br-PSAA solution for copper determination (R_{Cu}), 7×10^{-4} M 5-Br-PSAA solution for iron determination (R_{Fe}), 5×10^{-4} M ascorbic acid solution (AS) were aspirated from ports #1, #3, #4, and #6, respectively. Sample was aspirated from port #5. The third holding coil, HC_3 (1 mm i.d., 50 cm), connected to the port #2 was used to keep a spacer solution (SS_{Cu}, SS_{Fe} in Fig. 5-2) of 5×10^{-5} M 5-Br-PSAA in 0.01 M hydrochloric acid. The spacer solution in the HC_3 was aspirated from port #2 twice as described below. Diagram of sequence of reactant zones corresponding to one cycle of simultaneous determination of copper and iron is shown in Fig. 5-2. The SI-LOV protocol to carry out the sequence is shown in Table 5-1. At first, HC_1, HC_2, and HC_3 are filled with a carrier solution (CS, 5×10^{-5} M 5-Br-PSAA in 0.01 M hydrochloric acid), which is also used as SS_{Cu} and SS_{Fe}. The sample, reagents and SS_{Fe} for the

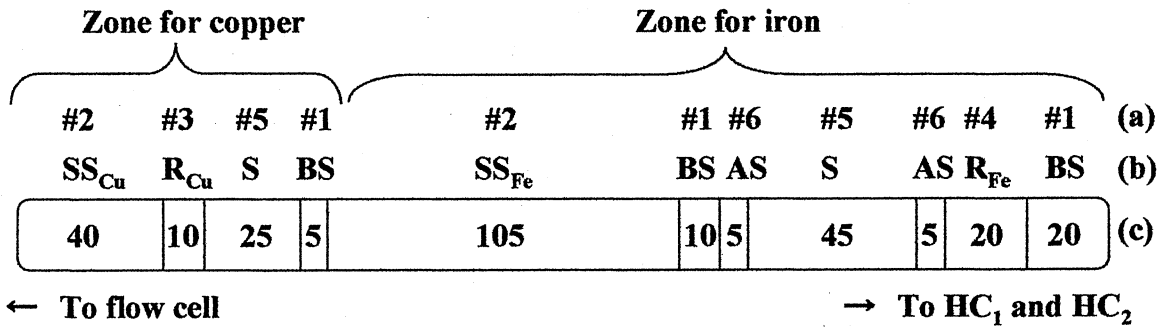

Fig. 5-2 Diagram of sequence by one cycle for the simultaneous determination of copper and iron. (a), Port numbers on lab-on-valve; (b), reagents aspirated (abbreviations are shown in Fig.5-1); (c), aspiration volume in μl.

determination of iron are aspirated from the respective ports (in the order: #1, #4, #6, #5, #6, #1, #2) into the HC_2. The sample, reagent and SS_{Cu} are then aspirated from corresponding ports port (in the order: #1, #5, #3, #2) into the HC_1. Thereafter the reaction products of Cu(II) and Fe(II) with 5-Br-PSAA are dispensed to the flow cell through the port#2 by reversing the direction of the flow. The role of the SS_{Cu} and SS_{Fe} is to promote efficient mixing of the sample and reagents in each zone before reaching the flow cell and also to completely separate the zones of Cu(II) and Fe(II) complexes that results in well separated detection peaks.

Table 5-1 SIA protocol for the simultaneous determination of copper and iron

SIA protocol	Note	SIA protocol	Note
		(1)	
Loop Start (#) 3			
syringe pump Valve In	Cleaning the whole flow line	Multiposition Valve acetate buffer	Aspiration of 0.2 M acetate buffer
syringe pump Flowrate (microliter/sec) 185		Syringe Pump Flowrate (microliter/sec) 15	
Syringe Pump Fill		Syringe Pump Aspirate (microliter) 10	
syringe pump Delay Until Done		Syringe Pump Delay Until Done	
Delay (sec) 1		Delay (sec) 2	
Multiposition Valve flow cell			
syringe pump Valve Out		Multiposition Valve flow cell	Aspiration of carrier solution
syringe pump Flowrate (microliter/sec) 185		Syringe Pump Flowrate (microliter/sec) 15	
syringe pump Dispense (microliter) 300		Syringe Pump Aspirate (microliter) 105	
Syringe Pump Delay Until Done		Syringe Pump Delay Until Done	
Delay (sec) 1		Delay (sec) 2	
Loop End			
Delay (sec) 2		Multiposition Valve acetate buffer	Aspiration of 0.2 M acetate buffer
		Syringe Pump Flowrate (microliter/sec) 15	
Multiposition Valve acetate buffer	Aspiration of 0.2 M acetate buffer	Syringe Pump Aspirate (microliter) 5	
Syringe Pump Flowrate (microliter/sec) 15		Syringe Pump Delay Until Done	
Syringe Pump Aspirate (microliter) 20		Delay (sec) 2	
Syringe Pump Delay Until Done			
Delay (sec) 2		Multiposition Valve sample (Cu)	Aspiration of copper solution at a suitable concentration
		Syringe Pump Flowrate (microliter/sec) 15	
Multiposition Valve 5-Br-PSAA	Aspiration of 7×10^{-4} M 5-Br-PSAA	Syringe Pump Aspirate (microliter) 25	
Syringe Pump Flowrate (microliter/sec) 15		Syringe Pump Delay Until Done	
Syringe Pump Aspirate (microliter) 20		Delay (sec) 2	
Syringe Pump Delay Until Done			
Delay (sec) 2		Multiposition Valve 5-Br-PSAA	Aspiration of 4×10^{-4} M 5-Br-PSAA
		Syringe Pump Flowrate (microliter/sec) 15	
Multiposition Valve ascorbic acid	Aspiration of 5×10^{-4} M ascorbic acid	Syringe Pump Aspirate (microliter) 10	
Syringe Pump Flowrate (microliter/sec) 15		Syringe Pump Delay Until Done	
Syringe Pump Aspirate (microliter) 5		Delay (sec) 2	
Syringe Pump Delay Until Done			
Delay (sec) 2		Multiposition Valve flow cell	Aspiration of carrier solution
		Syringe Pump Flowrate (microliter/sec) 15	
Multiposition Valve sample (Fe)	Aspiration of iron solution at a suitable concentration	Syringe Pump Aspirate (microliter) 40	
Syringe Pump Flowrate (microliter/sec) 15		Syringe Pump Delay Until Done	
Syringe Pump Aspirate (microliter) 45		Delay (sec) 2	
Syringe Pump Delay Until Done			
Delay (sec) 2		Multiposition Valve flow cell	
		Syringe Pump Flowrate (microliter/sec) 20	
Multiposition Valve ascorbic acid	Aspiration of 5×10^{-4} M ascorbic acid	Spectrometer Reference Scan	
Syringe Pump Flowrate (microliter/sec) 15		Spectrometer Absorbance Scanning	Absorbance monitoring starts.
Syringe Pump Aspirate (microliter) 5		syringe pump Dispense (microliter) 500	
Syringe Pump Delay Until Done		syringe pump Delay Until Done	
Delay (sec) 2		Spectrometer Stop Scanning	Absorbance monitoring stops.
		Loop End	
Continue to (1)		Stop program	

5.3. Results and Discussion

5.3.1. Peak profiles

Copper(II) and/or iron(II) reacts with 5-Br-PSAA to form red color chelate compound (Scheme 5-1).

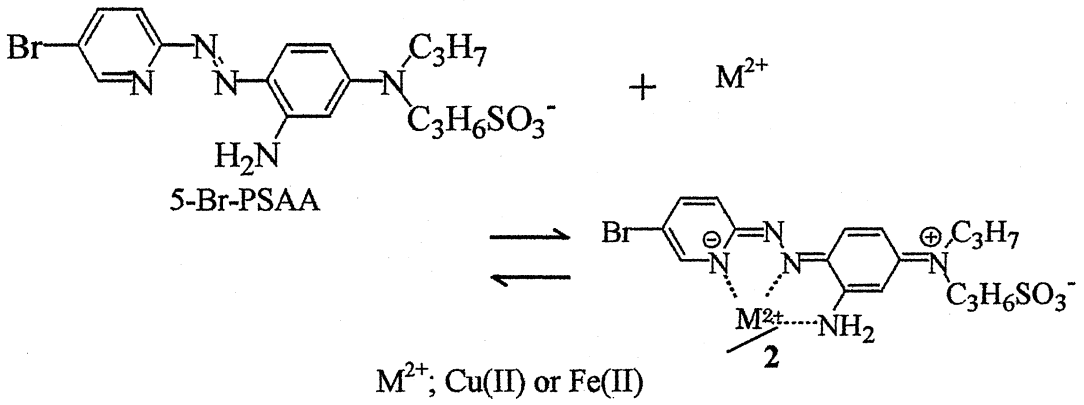

Scheme 5-1

However, copper(I) and iron(III) do not react with 5-Br-PSAA. The molar absorptivities for the copper(II)-5-Br-PSAA complex are 55000 l mol^{-1} cm^{-1} at 558 nm and 65000 l mol^{-1} cm^{-1} at 580 nm,[104] and those for the Fe(II) complex are 87000 l mol^{-1} cm^{-1} at 558 nm and 42000 l mol^{-1} cm^{-1} at 713 nm.[89] In this work, we chose the monitoring wavelengths of 580 nm for copper and 558 nm for iron, respectively, to ensure maximum sensitivity. Fig. 5-3 shows the peak profiles for Cu(II)- and Fe(II)-5-Br-PSAA complexes obtained by the proposed method. As shown in Fig. 5-2, there are two determination zones per one sequence; one zone containing SS_{Cu}, R_{Cu}, S, and BS in the HC_1 gives a first peak for copper, and another zone containing SS_{Fe}, BS, AS, S, and R_{Fe} in HC_2 gives a second peak for iron. When the sample solutions containing only copper

were introduced into the SI-LOV system, only first peak heights depended on the concentration of copper (Fig. 5-3 (a), (b), and (c)). On the other hand, the second peaks (Fig. 5-3 (a)', (b)', and (c)') were proportional to the concentration of iron. Hence, copper and iron can be determined simultaneously.

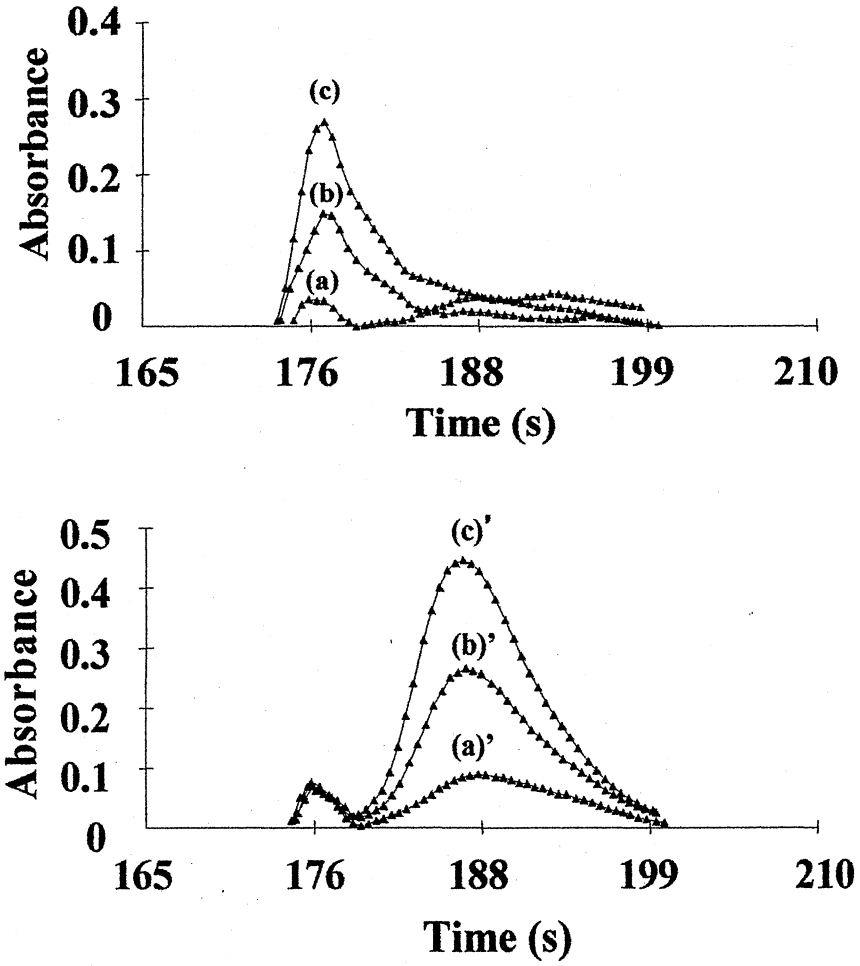

Fig. 5-3 Peak profiles obtained by the proposed method for copper at 580 nm and iron at 558 nm. (a), Blank for copper; (b), 0.5 ppm copper; (c), 1 ppm copper; (a)', blank for iron; (b)', 0.5 ppm iron; (c)', 1 ppm iron. Other conditrons are the same as in Fig. 5-1.

5.3.2. *Effects of 5-Br-PSAA concentrations*

Fig. 5-4 shows the effect of 5-Br-PSAA concentration in R_{Cu} and R_{Fe} on the color development with 1 ppm copper and 1 ppm iron. The concentrations were varied from 1×10^{-4} to 5×10^{-4} M for copper and from 2×10^{-4} to 1×10^{-3} M for iron. The net absorbance of the copper complex was almost constant over the examined range and that of iron complex was monotonically increased with an increase in 5-Br-PSAA concentration. Both of the blank peaks for copper and iron also increased with an increase in 5-Br-PSAA concentration. We chose therefore 5-Br-PSAA concentrations of 4×10^{-4} M for copper and 7×10^{-4} M for iron.

5.3.3. *Effect of 5-Br-PSAA concentration in carrier solution*

Fig. 5-5 shows the effects of 5-Br-PSAA concentration in carrier solution, which was used as SS_{Cu} and SS_{Fe} to suppress the high reagent blank. The 5-Br-PSAA concentration was varied from 0 to 1×10^{-4} M. The blank peaks for copper and iron favorably decreased with an increase in the concentration of 5-Br-PSAA, because the 5-Br-PSAA concentration gap between R_{Cu} or R_{Fe} and the carrier solution was narrowed. At the same time, the net absorbance for copper increased with increasing the reagent concentration up to 2×10^{-5} M, and that for iron also increased over the range examined. These results indicated that 5-Br-PSAA in SS_{Cu} and SS_{Fe} suppressed each blank and that promoted the complex formations. Thus, a 5×10^{-5} M of 5-Br-PSAA in 0.01 M hydrochloric acid was chosen as SS_{Cu} and SS_{Fe}.

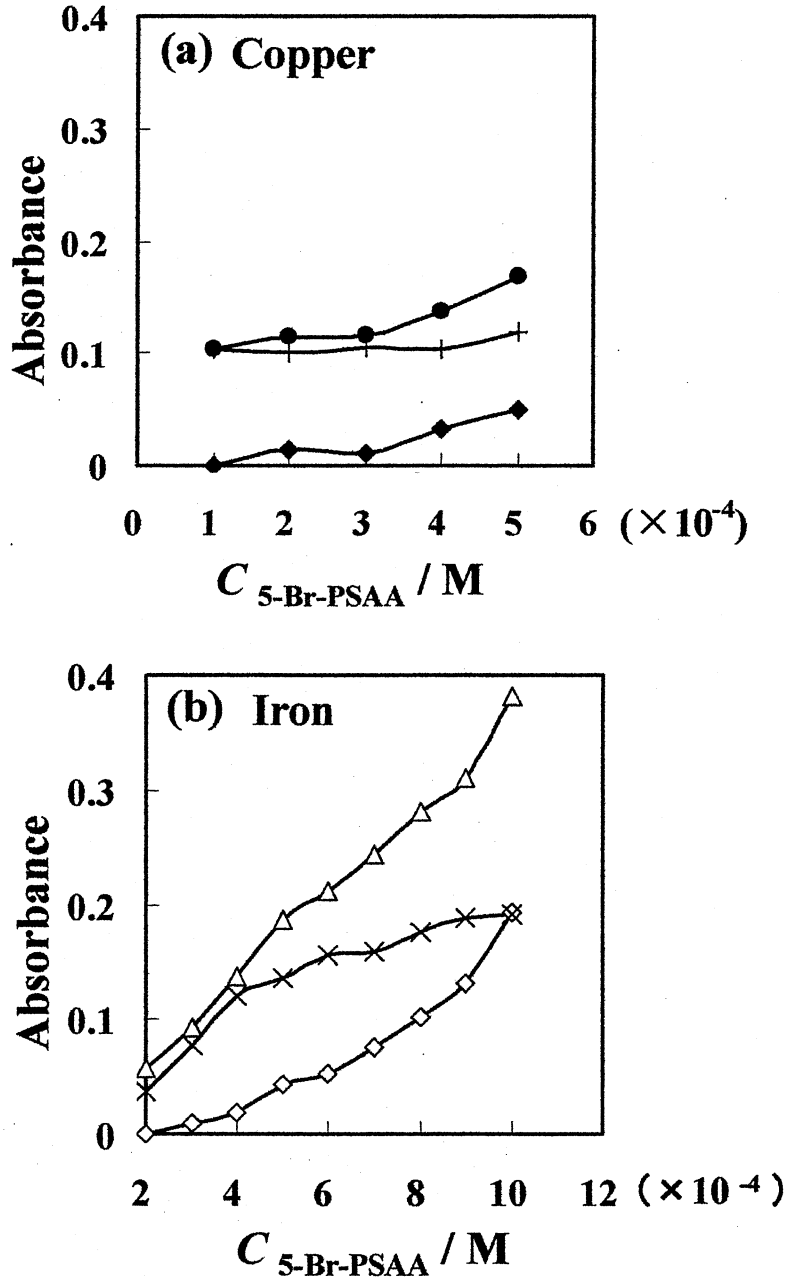

Fig. 5-4 Effects of 5-Br-PSAA concentration on the (a) copper and (b) iron determination. (◆), blank for copper; (●), 1 ppm copper; (+), net; (◇), blank for iron; (△), 1 ppm iron; (×), net. Other conditions are the same as in Fig. 5-1.

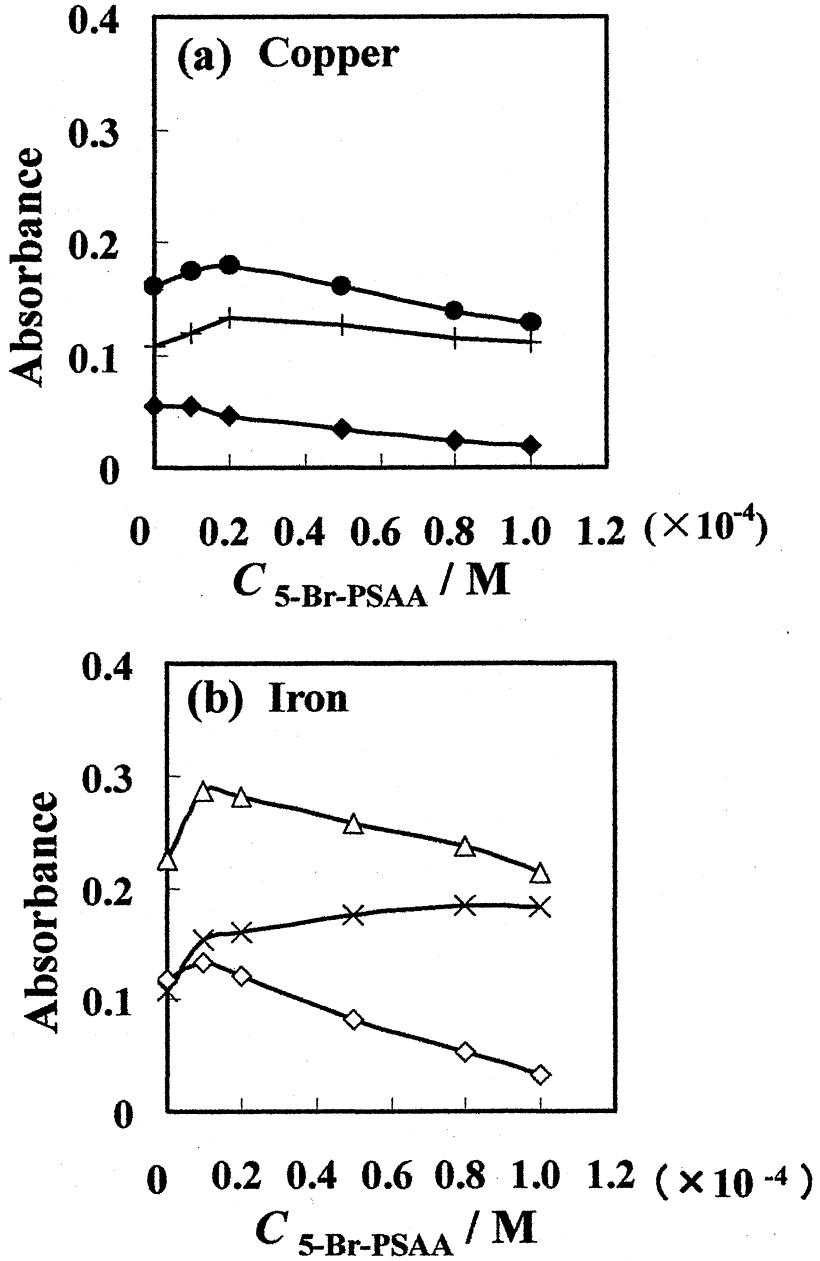

Fig. 5-5 Effects of 5-Br-PSAA concentration in carrier used as spacer on the (a) copper and (b) iron determination. (◆), blank for copper; (●), 1 ppm copper; (+), net; (◇), blank for iron; (△), 1 ppm iron; (×), net. Other conditions are the same as in Fig. 5-1.

5.3.4. Effect of pH

The effects of the reaction pH with acetate buffer were studied in the pH range 3.8 to 5.0 on the copper and iron determinations. As can be seen in Fig. 5-6, no colored complex of iron was produced at pH 3.9. The peak heights for copper and iron were maximum and essentially constant over the pH range 4.6 – 5.0. Thus, acetate buffer solution (pH 4.6) was used for the simultaneous determination of copper and iron.

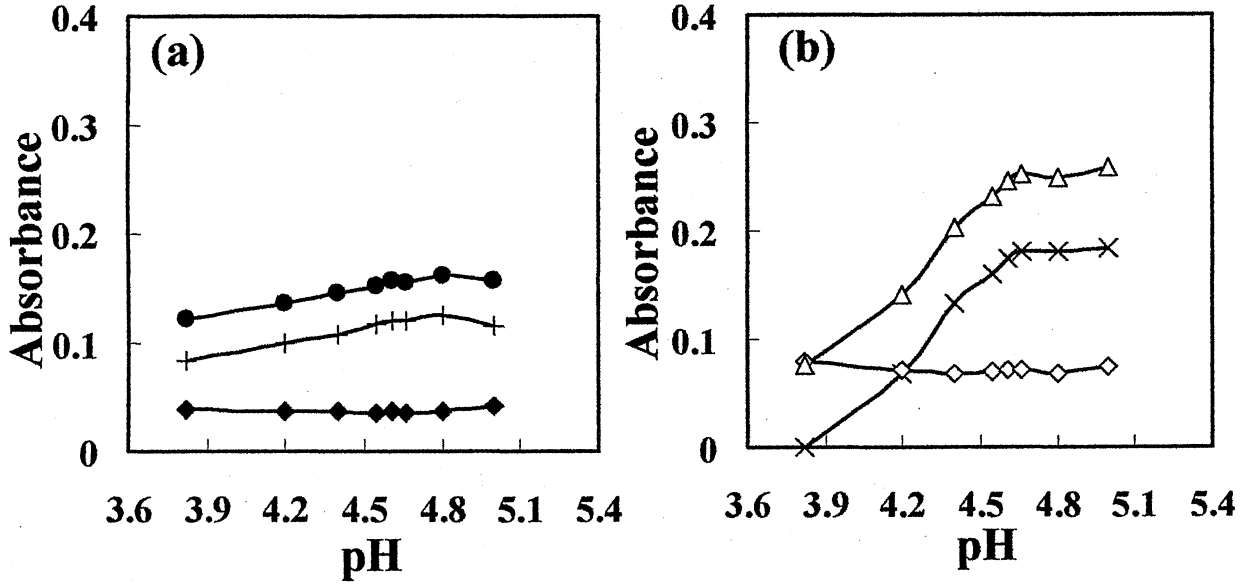

Fig. 5-6 Effects of pH on the (a) copper and (b) iron determination. (◆), blank for copper; (●), 1 ppm copper; (+), net; (◇), blank for iron; (△), 1 ppm iron; (×), net. Other conditions are the same as in Fig. 5-1.

5.3.5. *Effect of ascorbic acid concentration on iron determination*

Ascorbic acid was used to reduce iron(III) to iron(II) and also to protect the peak for iron from the interference of copper(II) since the copper(II)-5-Br-PSAA complex can be decomposed by this reductant.[105] Therefore, sample in the iron determination zone was sandwiched between two zones of ascorbic acid solutions as shown in Fig. 5-2. Ascorbic acid concentration was varied from 0 to 1×10^{-3} M. In the absence of ascorbic acid, an undesirable peak was obtained, *i.e.* copper(II) reacted with 5-Br-PSAA in the SS_{Fe}. When the ascorbic acid concentration was over 1×10^{-4} M, the interference from copper(II) was removed, and the peak for iron was maximum and constant. A 5×10^{-4} M ascorbic acid was thus selected for the iron determination.

5.3.6. *Effect of reaction temperature on iron determination*

The effect of the temperature on the complex-formation reaction of iron with 5-Br-PSAA was studied in the range from 25 to 50°C. The reaction was accelerated by increasing the temperature up to 40°C and the absorbance was maximum and constant over the range from 40 to 50°C. Thus the optimum reaction temperature for the determination of iron was 45°C.

5.3.7. *Effects of aspiration volumes*

The effects of aspiration volumes of spacers, sample, and reagents were studied with test solutions containing 1 ppm copper and 1 ppm iron. In

these optimizations, another volume of SS_{Cu} or SS_{Fe} was simultaneously varied together with the other parameter optimized to maintain constant overall volume of the sequence of zones corresponding to the peak of the another analyte (so that the distance between the colored product zone and the flow cell is not changed). For instance, when the volume of R_{Cu} was increased by 10 µl during the R_{Cu} optimization, the volume of SS_{Fe} was reduced by 10 µl. Otherwise the travel path of the iron zone to the flow cell would increase, in other words the dispersion of the iron zone would increase. In this case, the compensation kept the peak height for iron constant even if the volume of R_{Cu} was varied. When applying such volume compensation, in all cases the changes of volume in the copper detectable zone did not also affect the peak heights of iron and *vice versa.* In the following discussion, we focus on the effects of aspiration volumes on either copper or iron determination.

5.3.8. Effects of sample volumes

The sample volume in the copper zone was varied from 15 to 35 µl. The net absorbance at 580 nm linearly increased with increasing the sample volume. The sample volume in the iron zone was varied from 35 to 50 µl. At a sample volume over 45 µl, the net absorbance at 558 nm was almost constant. The blank values for copper and iron were constant. Thus, the optimum sample volumes were selected to be 25 µl for copper and 45 µl for iron.

5.3.9. Effects of reagent volumes

5-Br-PSAA is a sensitive chromogenic reagent for the determination of iron(II),[92] cobalt(III),[92] copper(II),[92,104] nickel(II),[92,106] and palladium(II)[107]. Nevertheless, this reagent is expensive and therefore, reasonable volume reduction consumed is desirable. The effects of 5-Br-PSAA volumes were investigated from 5 to 20 μl for R_{Cu} and from 10 to 35 μl for R_{Fe}. Although the peak heights for copper and iron increased with an increase in the volumes of R_{Cu} and R_{Fe}, the blank absorbances increased, too. Taking into account the sensitivity and the blank absorbance, the optimum volumes of R_{Cu} and R_{Fe} were selected to be 10 and 20 μl, respectively. The volumes of two AS zones were individually varied from 5 to 15 μl; optimum values were 5 μl of each. Optimizations for the BS volumes in both copper and iron zones were also carried out, and the optimum volumes are shown in Fig. 5-2.

5.3.10. Effects of spacer solutions volumes

The effect of SS_{Cu} volume on the determination of 1 ppm copper was studied over the range from 20 to 50 μl. The net absorbance was constant in the examined range, but smaller SS_{Cu} resulted in high blank because the R_{Cu} got much closer to the flow cell. We chose therefore the SS_{Cu} of 40 μl. When varying the SS_{Fe} volume from 0 to 140 μl, the net absorbance of iron was also constant. Similarly, considerable small SS_{Fe} resulted in high blank and poor peak separation; thus SS_{Fe} of 105 μl was chosen.

5.3.11. Calibration graphs

Calibration graphs for copper and iron under the optimum conditions are shown in Fig. 5-7. The calibration graphs were linear for 0.1 – 2 ppm copper ($r^2 = 0.997$) and 0.1 – 5 ppm iron ($r^2 = 0.999$), respectively:

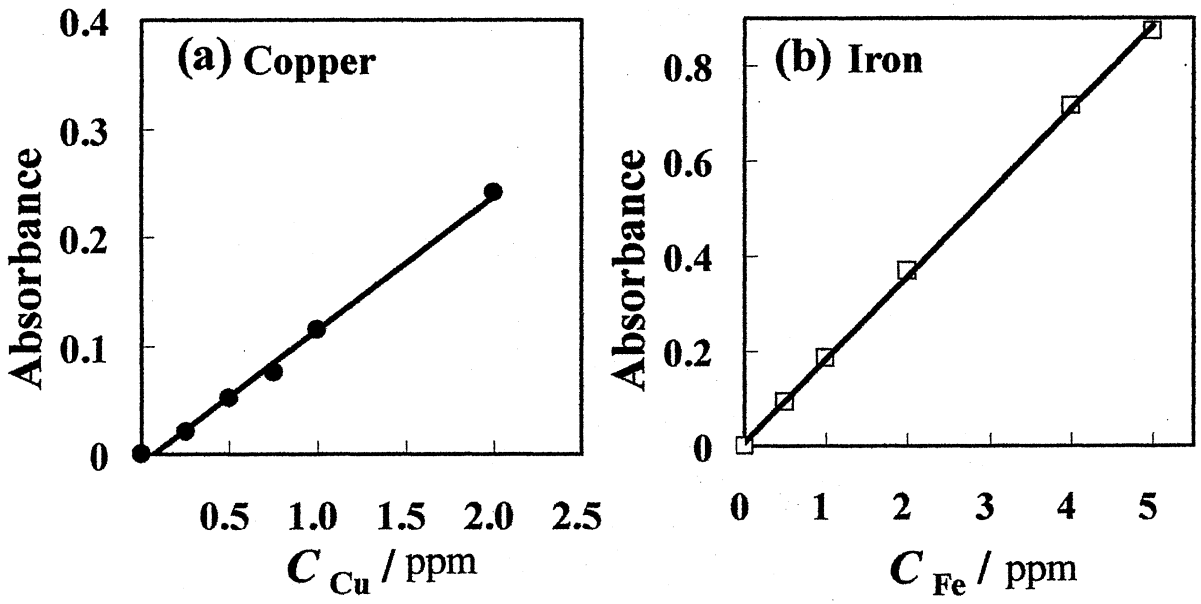

Fig. 5-7 Calibration curves for (a) copper and (b) iron.

Net absorbance for copper = $(1.22 \pm 0.02)\times10^{-1}$[copper, ppm]

$-(9 \pm 2)\times10^{-3}$ ..... (1)

Net absorbance for iron = $(1.73 \pm 0.02)\times10^{-1}$[iron, ppm]

$+(6 \pm 10)\times10^{-3}$ ..... (2)

With replicate sample injections, the relative standard deviations (RSD) (n = 15) of peak heights were 2% and 1.9% (for 0.5 and 1 ppm copper, respectively) and the RSDs for 0.5 and 1 ppm iron were 1.8% and 1.2%.

The detection limits (3σ) were 50 ppb for copper and 25 ppb for iron. The sampling rate was 18 sample h^{-1} for the simultaneous analysis.

Copper and iron in artificial mixtures with some known concentrations were determined. The concentration ranges were 0.25 – 2 ppm for copper and 0.25 – 5 ppm for iron (the Cu/Fe ratios were 1:10 to 5:1). The results are represented in Table 5-2. The recoveries of both analytes were 96 – 105%.

Table 5-2 Simultaneous determination of copper and iron in artificial mixtures

Added/ppm		Found [a] / ppm		Recovery / %	
Cu	Fe	Cu	Fe	Cu	Fe
0.25	0.25	0.24±0.01	0.24±0.00	97	97
0.5	0.5	0.48±0.01	0.51±0.01	96	102
1	1	1.02±0.01	1.01±0.01	102	101
0.5	0.25	0.50±0.02	0.24±0.01	100	97
0.5	1	0.49±0.02	1.02±0.01	97	102
0.5	2	0.51±0.01	1.99±0.01	102	100
0.5	5	0.51±0.02	5.04±0.04	102	101
1	0.2	1.01±0.01	0.21±0.00	101	105
1	0.5	1.01±0.02	0.52±0.01	101	104
2	0.5	2.05±0.01	0.50±0.01	103	99

a Average value for three determinations.

5.3.12. Interference study

The interferences of foreign ions on the determination of a mixture of 0.5 ppm copper(II) and 0.5 ppm iron(III) were studied. The results are summarized in Table 5-3. An error of less than ±5% was considered to be

tolerable on each peak height. Most of the metal ions and inorganic anions did not interfere at levels from 5 to 5000 ppm. But the tolerance limits of some metals such as cobalt(II), palladium(II) and nickel(II) were low due to the complex formations with 5-Br-PSAA. 0.1 ppm cobalt(II), 0.2 ppm palladium(II) and 0.2 ppm nickel(II) gave some interferences.

Table 5-3 Interference of foreign ions on the simultaneous determination of 0.5 ppm copper and 0.5 ppm iron

Tolerance limit / ppm	Ion added[a]	
	For copper determination	For iron determination
5000	Na, K, Zn(II), Pb(II), Cd(II), Cl^-, NO_3^-, Br^-, SO_4^{2-}	Na, Cl^-, NO_3^-, Br^-, SO_4^{2-}
2000	Mn(II), Ca(II)	K, Pb(II)
1000	Al(III)	Mn(II), Ca(II)
500	Mg(II)	Mg(II), Zn(II), Cd(II)
200		Al(III)
50	Mo(IV), Sn(II), Se(IV)	Se(IV), V(V)
20		Mo(IV)
10	V(V)	
5		Sn(II)
2	Ni(II)	Pd(II)
0.2	Pd(II)	Ni(II)
0.1	Co(II)	Co(II)

[a] An error of 5% is considered to be tolerable.

5.3.13 Applications

The proposed SI-LOV method was applied to the simultaneous determination of copper and iron in multi-element solution with certified values (Table 5-4). After the original solution (5 or 6 ml) was neutralized, the solution was diluted to 100 ml with 0.01 M hydrochloric acid. The analytical values obtained by the proposed method were in good agreement

with the certified values. In addition, the proposed method was applied to industrial wastewater sample analysis. As can be seen in Table 5-5, there is no significant difference between the results obtained by the proposed SIA-LOV method and those by ICP-AES, which is demonstrated by acceptable *t*-test values.

Table 5-4 Simultaneous determination of copper and iron in multi-element standard for ICP spectroscopy

Found / ppm		Certified value / ppm	
Cu	Fe	Cu	Fe
10 ± 0.4 [a]	31 ± 0.3 [a]	10	30
10 ± 0.3 [b]	30 ± 0.4 [b]		

[a] After neutralizing 6 ml of original solution, the solution was diluted to 100 ml with 0.01 M HCl.

[b] After neutralizing 5 ml of original solution, the solution was diluted to 100 ml with 0.01 M HCl.

Table 5-5 Simultaneous determination of copper and iron in industrial wastewater[a]

Sample	SIA method / ppm		ICP-AES / ppm	
	Cu	Fe	Cu	Fe
1[b]	1.12±0.05	2.86±0.06	1.1	2.9
2[c]	1.98±0.02	7.00±0.04	1.9	6.9
3[d]	0.79±0.02	0.46±0.02	0.81	0.46
4[e]	1.90±0.04	0.98±0.05	1.8	0.98
5[f]	0.74±0.02	0.44±0.02	0.83	0.48

[a] t_{exp} for Cu: 0.284; t_{exp} for Fe: 0.156; t (95%): 2.776.

[b, d, f] After 5 ml of each sample solution was neutralized, it was placed in a 10 ml volumetric flask with 0.01 M HCl.

[c, e] After 2.5 ml of each sample solution was neutralized, it was placed in a 10 ml volumetric flask with 0.01 M HCl.

5.4. Conclusion

We proposed here an affordable and precise SI-LOV system with 5-Br-PSAA for the simultaneous spectrophotometric determination of copper and iron. The use of spacer containing the chromogenic reagent resulted in the suppression of blank, the promotion of the complex formation reaction and the successful separation of peaks for copper and iron. The proposed SI-LOV method has wide determinable ranges from 0.1 to 2 ppm for copper and from 0.1 to 5 ppm for iron, respectively, with low RSD values and low reagent consumption. the computer-controlled SI-LOV system is suitable for performing routine automated assays of copper and iron in wastewater.

Chapter 6 Conclusions

Although ICP-AES and ICP-MS are often used for the simultaneous determination of trace amounts of heavy metals, these instruments are expensive and the high skill is required. So, the cost performance analytical techniques are desired for the sensitive determination of heavy metals. The catalytic spectrophotometry with oxidation-reduction of metal ions is available for enhancement of sensitivity. In this study, the coupling reaction with *p*-anisidine and *N,N*-dimethylaniline in the presence of Cu(II) and Fe(III) was investigated by the batchwise procedure. Addition of some activators (neocuproine for copper and 1,10-phenanthroline for iron) accelerated the reaction rate. The method could be successfully applied to the analyses of copper and iron at sub-ppb level in tap and natural waters without preconcentration and separation. The cyclic redox reaction metioned above was introduced to the FIA system. In the FIA system, a serial flow cell designed by the co-workers was used for simultaneous determination of trace amounts of copper and iron. The FI method was also applied to the assay of labile and inert complexes with humic acid for the characterization of copper- and iron complexes. In addition, the sensitive and rapid FI spectrophotometric method using the redox reaction of Co(II) with Fe(III) in the presence of nitro-PAPS was investigated. The proposed method was applied to the determination of cobalt in cobalt alloy, pepperbush leaves and Vitamine B_{12}. Finally, SIA method using the chromogenic reagent, 5-Br-PSAA, was investigated for the successive determination of copper and iron. The computer-controlled SI-LOV was assembled as the automated analyzer. The system was useful on the routine, durable and automated assay of copper and iron in the industrial waste

waters. The flow-based analytical techniques with FIA and SI-LOV should be noticed as an environmental benign technology.

References

1. T. Kawashima, N. Teshima, S. Nakano: "Catalytic Kinetic Determinations: Nonenzymatic," in "*Encyclopedia of Analytical Chemistry: Applications, Theory and Instrument,*" Vol. 12, Edited by Robert A. Meyers, p. 11034, **2000**, John Wiley&Sons, Chichester.
2. T. Kawashima, H. Itabashi, N. Teshima, M. Kurihara, S. Nakano, *Anal. Sci.*, **1999**, 15, 835.
3. S. Nakano, K. Tshijii, T. Kawashima, *Talanta*, **1995**, 42, 1051.
4. S. Nakano, K. Tanaka, R. Oki, T. Kawashima, *Talanta*, **1999**, 49, 1077.
5. Z. Yu, N. Teshima, S. Nakano, T. Kawashima, Talanta, **1996**, 43, 1519.
6. J. Ruzicka, E. H. Hansen, *Anal. Chim. Acta*, **1975**, 78, 145.
7. J. Ruzicka: "SEQUENTIAL INJECTION FOR BIOMOLECULAR ASSAYS", e-monograph CD-ROM, (**2004**), published by FIAlab Instruments, inc.
8. T. Sakai, Y. Maeda, N. Ura, *Talanta*, **1999**, 49, 989.
9. T. Sakai, A. Yanagisawa, K. Higuchi, N. Teshima, N. Ura, *Talanta*, **2000**, 52, 159.
10. T. Sakai, *J. Flow Injection Anal.*, **2000**, 17, 156.
11. N. Teshima, T. Nobuta, T. Sakai, *Anal. Chimi. Acta*, **2001**, 438, 21.
12. E. P. Serjeant, "Potentiometry and Potentiometric Titrations", in " A Series of Monographs on Analytical Chemistry and Its Applications " vol. 69, p 38, **1984**, John Wiley and Sons, New York.
13. J. Ruzicka, G. D. Marshall, *Anal. Chem. Acta*, **1990**, 237, 329.

14. J. F. van Staden, A. Botha, *Talanta*, **1999**, 49, 1099.
15. Ludwig V. Mulaudzi, Jacobus F. van Staden, Raluca I. Stefan, *Anal. Chim. Acta*, **2002**, 467, 35.
16. R. E. Taljaard, J. F. van Staden, *Anal. Chimi. Acta*, **1998**, 366, 177.
17. Rui Cerdeira C. Costa, Ml Isabel Cardoso, and Alberto N. Araujo, *Am. J. Enol. Vitic.*, **2000**, 51, 131.
18. Yongyi Luo, Shigenori Nakano, David A. Holman, Jaromir Ruzicka, Gary D. Christian, *Talanta*, **1997**, 44, 1563.
19. J. Ruzicka, E. H. Hansen, *Anal. Chem.*, **2000**, 72, 212A.
20. S. Ohno, N. Teshima, H. Zhang, and T. Sakai, *Talanta*, **2003**, 60, 1177.
21. J. H. Martin, S. E. Fitzwater, *Nature*, **1988**, 331, 341.
22. K. H. Coale, Limnol. Oceanogr. **1991**, 36, 1851.
23. J. B. Sprague, *Nature*, **1968**, 220, 1345.
24. S. Nakano, *Bunseki Kagaku*,**1999**, 48, 285.
25. T. Kawashima, N. Teshima, S. Nakano, "*Catalytic Kinetic-Determinations: Nonenzymatic in Encyclopedia of Analytical Chemistry*", ed. R. A. Meyers, pp. 11034-11070. John Wiley & Sons, Chichester, **2000**.
26. S. R. Crouch, A. Scheeline and E. S. Kirkor, *Anal. Chem*, **2000**, 72, 53R.
27. S. Kawakubo, Y. Hagihara, Y. Honda and M. Iwatsuki, *Anal. Chim. Acta*, **1999**, 388, 35.
28. S. Kawakubo and M. Iwatsuki, *Anal. Sci.*, **2000**, 16, 945.
29. J. Wang and R. He, *Anal. Chim. Acta*, **1994**, 294, 195.
30. Z. Zhu, C. Han , Z. Gu and R. Chen, *Analyst*, **1994**, 119, 2251.
31. W. Jianhua and H. Ronghuan, *Mikrochim. Acta*, **1994**, 117, 23.

32. C. G. Papadopoulos and A. C. Zotou, *Mikrochim. Acta*, **1992**, 106, 203.
33. W. Jianhua and H. Ronghuan, *Anal. Chim. Acta*, **1995**, 303, 241.
34. R. Liu, D. Liu, A. Sun and G. Liu, *Analyst*, **1995**, 120, 565.
35. T. Tomiyasu, *Anal. Chim. Acta*, **1997**, 349, 43.
36. Z. Zhu, Z. Gu , R. Chen, C. Han and B. Lu, *Anal. Chim. Acta*, **1994**, 298, 19.
37. Y.-Z. Ye, H.-Y. Mao and Y.-H. Chen, *Talanta*, **1998**, 45, 1123.
38. S. Nakano, K. Kuramono and T. Kawashima, *Chem. Lett.*, **1980**, 849.
39. T. Kawashima, Y. Kozuma and S. Nakano, *Anal. Chim. Acta*, **1979**, 106, 355.
40. P. R. Bontchev, *Talanta*, **1972**, 19, 675.
41. T. Watanabe, N. Teshima, M. Kurihara, S. Nakano and T. Kawashima, *Chem. Lett*, **1999**, 521.
42. W. A. E. McBryde, A Critical Review of Equilibrium Data for Proton- and Metal Complexes of 1,10-phenanthroline, 2,2'-Bipyridyl and Related Compounds, Pergamon Press, Oxford (**1978**).
43. L. G. Sillen, Stability Constants of Metal-Ion Complexes, Section I: Inorganic Ligands, The Chemical Sciety, Burlington House (**1964**).
44. S. Ohno, M. Tanaka, N. Teshima, and T. Sakai, *Anal. Sci.*, **2004**, 20, 171.
45. J. Wei, N. Teshimia, S. Ohno, and T. Sakai, *Anal. Sci.*, **2003,** 19, 731.
46. T. M. Florence and G. E. Batley, *Talanta*, **1977**, 24, 151.
47. Y. Miyata, T. Hirano, S. Nakano, and T. Kawashima, *Anal. Sci.*, **1991**, 7, 97.

48. S. Nakano, S. Hinokuma, and T. Kawashima, *Chem. Lett.*, **1983**, 357.
49. S. Nakano, M. Tago, and T. Kawashima, *Anal. Sci.*, **1989**, 5, 69.
50. S. Ohno, N. Teshima, T. Watanabe, H. Itabashi, S. Nakano, and T. Kawashima, *Analyst*, **1996**, 121, 1515.
51. T. Tomiyasu, N. Yoonehara, N. Teshima, and T. Kawashima, *Anal. Chim. Acta*, **1999**, 394, 55.
52. G. Scarano, E. Morelli, A. Seritti, and A. Zirino, *Anal. Chim. Acta*, **1990**, 62, 943.
53. K. Yokoi, T. Tomisaki, T. Koide, and C. M. G. van den Berg, *Fresenius' J. Anal. Chem.*, **1995**, 352, 547.
54. S. Gotoh, N. Teshima, T. Sakai, K. Ida, and N. Ura, *Anal. Chim. Acta*, **2003**, 499, 91.
55. S. Nakano, K. Kuramoto and T. Kawashima, *Chem. Lett.*, **1980**, 849.
56. M. Tanaka, Y. Watanabe, S. Ohno, T. Tamaru, N. Teshima, and T. Sakai, *Bunseki kagaku*, **2004**, 53, 291.
57. I. V. Pyatnitskii, Analytical Chemistry of Cobalt
58. J. A. Disegi, R. L. Kennedy, R. Pilliar, "*Cobalt-Base Alloys for Biomedical Applications*", **1990**, American Society for Testing and Materials.
59. T. Sakai, N. Ohno, H. Sasaki, *Bunseki Kagaku*, **1991**, 40, 305.
60. G. F. Combs, Jr. "*The Vitamins, Fundamental Aspects in Nutrition, and Health*" 2 nd edition, **1998**, Academic Press. San Diego.
61. The Japan Society for Analytical Chemistry "Bunseki kagaku data book" 4 th edition (**1994**) Maruzen.
62. H. Tanaka, H. Morita, S. Shimomura, K. Okamoto, *Anal. Sci.*, **1997**, 13, 607.

63. F. Vydra, R. Pribil, *Talanta*, **1959**, 3, 103.
64. F. Vydra, R. Pribil, *Talanta*, **1960**, 5, 44.
65. N. Teshima, T. Kawashima, *Bull. Chem. Soc. Jpn.*, **1996**, 69, 1997.
66. H. Katsumata, N. Teshima, T. Kawashima, *Anal. Sci.*, **1997**, 13, 825.
67. H. Katsumata, N. Teshima, T. Kawashima, *Bull. Chem. Soc. Jpn.*, **1997**, 70, 2151.
68. M. Saito, D. Horiguchi, K. Kina, *Bunseki kagaku*, **1981**, 30, 635.
69. T. Makino, M. Kiyonaga, K. Kina, *Clin. Chim. Acta*, **1988**, 171, 19.
70. T. Makino, *Clin. Chim. Acta*, **1991**, 197, 209.
71. N. Ohno, T. Sakai, *Bunseki kagaku*, **1997**, 46, 937.
72. C. Ohtsuka, K. Matsuzawa, H. Wada, G. Nakagawa, *Anal. Chim. Acta*, **1992**, 256, 91.
73. T. Okutani, Y. Tsukada, A. Sakuragawa, T. Yamaji, S. Morita, *J. Chromatogr. A*, **1997**, 788, 113.
74. C. Ohtsuka, Y. Mori, S. Hayashi, T. Tsuda, H. Wada, *J. Liq. Chrom. &Rel. Technol.*, **2000**, 23, 669
75. T. Yamane, H. Yamada, *Anal. Chim. Acta*, **1995**, 308, 433.
76. T. Yamane, Y. Yamaguchi, *Mikrochim. Acta*, **1998**, 130, 111.
77. S. Ohno, N. Teshima, T. Sakai, K. Grudpan, M. Polasek, *Talanta*, **2006**, 68, 527.
78. T. Tsuzuki, Y. Itoh, Y. Ueda, "*Water and Water Pollution*" (in Japanese), ed. M. Taga, M. Kataoka, S. Tanaka, Sankyo Shuppan, Tokyo, **1997**, 19.
79. R. Eife, M. Weiss, J. Muller-Hocker, T. Lang, V. Barros, B. Sigmund, F. Thanner, P. Welling, H. Lange, W. Wolf, B. Rodeck, J. Kittel, P. Schramel, K. Reiter, *Eur. J. Med. Res.*, **1999**, 4, 224.
80. T. Kowalczyk, A. L. Pope, D. K. Sorensen, D. K., *J. Am. Vet. Med. Assoc.*, **1962**, 141, 362.

81. V. Cheevaporn, P. Menasveta, *Mar. Poll. Bull.*, **2003**, 47, 43.
82. http://law.e-gov.go.jp/htmldata/S46/S46F03101000035.html
83. JIS K 0102, "*Testing Method for Industrial Wastewater*" Japanese Industrial Standards Committee (**1998**).
84. K. Toda, *Bunseki Kagaku*, **2004**, 53, 207.
85. M. Miro, J. M. Estela, V. Cerda, *Talanta*, **2003**, 60, 867; **2004**, 62, 1; **2004**, 63, 201.
86. T. Yao, *J. Flow Injection Anal.*, **2004**, 21, 59.
87. H. Ukeda, *Bunseki Kagaku*, **2004**, 53, 221.
88. P. Solich, H. Sklenarova, M. Polasek, R. Karlicek, *J. Flow Injection Anal.*, **2001**, 18, 13; **2001**, 18, 118.
89. N. Ohno, T. Sakai, *Bunseki Kagaku*, **1998**, 47, 795.
90. N. Ohno, T. Sakai, *Bunseki Kagaku*, **2004**, 53, 233.
91. S. Gotoh, N. Teshima, T. Sakai, K. Ida, N. Ura, *Ana. Chim. Acta*, **2003**, 499, 91.
92. D. Horiguchi, M. Saito, K. Noda, K. Kina, *Anal. Chim. Acta*, **1983**, 151, 457.
93. C. E. Lenehan, N. W. Barnett, S. W. Lewis, *Analyst*, **2002**, 127, 997.
94. V. P. Andreev, N. B. Ilyna, D. A. Holman, L. D. Scampavia, G. D. Christian, *Talanta*, **1999**, 48, 485.
95. E. Rubi, R. Forteza, V. Cerda, *Lab. Rob. Autom.*, **1996**, 8, 149.
96. J. A. Vieira, J. I. M. Raimundo, B. F. Reis, E. A. G. Zagatto, J. L. F. C. Lima, *Anal. Chim. Acta*, **1998**, 366, 257.
97. T. McCormack, J. F. van Staden, *Anal. Chim. Acta*, **1998**, 367, 111.
98. F. Mas, A. Cladera, J. M. Estela, V. Cerda, *Analyst*, **1998**, 123, 1541.

99. A. Cladera, C. Tomas, E. Gomez, J. M. Estela, V. Cerda, *Anal. Chem. Acta*, **1995**, 302, 297.

100. J. M. Estela, A. Cladera, A. Munoz, V. Cerda, *Int. J. Environ. Anal. Chem.*, **1996**, 64, 205.

101. J. de Gracia, M. L. M. F. S. Saravia, A. N. Araujo, J. L. F. C. Lima, M. del Valle, M. Poch, *Ana. Chim. Acta*, **1997**, 348, 143.

102. S. Suteerapataranon, J. Jakmunee, Y. Vaneesorn, K. Grudpan, *Talanta*, **2002**, 58, 1235.

103. S. Nishihama, L. Scampavia, J. Ruzicka, *J. Flow Injection Anal.*, **2002**, 19, 19.

104. T. Makino, *Clin. Chim. Acta*, **1989**, 185, 7.

105. S. W. Kang, T. Sakai, N. Ohno, *Anal. Chim. Acta*, **1992**, 261, 197.

106. N. Ohno, T. Sakai, M. Nakabayashi, H. Sasaki, *Bunseki Kagaku*, **1990**, 39, 399.

107. T. Sakai, N. Ohno, *Anal. Chim. Acta*, **1988**, 214, 271.

Acknowledgment

I deeply wishes to express his sincere thanks to Professor Tadao Sakai and Associate Professor Norio Teshima for many useful advices and valuable discussions. Also, I appreciate Professor Shinji Inagaki and Professor Shin Tsuge of Department of Applied Chemistry, Aichi Institute of Technology for useful suggestion on this research.

I express my deepest appreciation to Professor Kate Gudpan of Department of Chemistry, Faculty of Science, Chiang Mai University in Thailand and Professor Miroslav Polasek of Department of Analytical Chemistry, Faculty of Pharmacy, Charles University in Czech Republic.

The author is also grateful to Dr. Heng Zhang of Industry School of Huaiyin in China and Dr. Jiatai Wei of Department of Environment Engineering, Faculty of Civil Engineering, Southeast University in China.

Sincere thanks are due to Mrs. Miho Horikiri, Mr. Yasuyuki Watanabe and Mr. Takaomi Tamaru who carried out experiments to prepare this doctoral thesis.

List of publications

1. Shinsuke Ohno, Norio Teshima, Heng Zhang and Tadao Sakai
   Utilization of activating and masking effects by ligands for highly selective catalytic spectrophotometric determination of copper and iron in natural waters, *Talanta*, **2003**, 60, 1177-1185
2. Jiatai Wei, Norio Teshimia, Shinsuke Ohno, and Tadao Sakai
   Catalytic Flow-Injection Determination of Sub-ppb Copper(II) Using the Redox Reaction of Cysteine with Iron(III) in the Presence of 2,4,6-Tris(2-pyridyl)-1,3,5-triazine, *Anal. Sci.*, **2003,** 19, 731-735
3. Shinsuke Ohno, Miho Tanaka, Norio Teshima, Tadao Sakai
   Successive Determination of Copper and Iron by a Flow Injection Catalytic Photometric Method Using a Serial Flow Cell, *Anal. Sci.*, **2004**, 20, 171-175
4. 田中美穂，渡辺靖之，大野慎介，田丸貴臣，手嶋紀雄，酒井忠雄
   コバルト(II)による鉄(III)の還元反応に及ぼす Nitro-PAPS の効果とそれを利用するコバルト(II)のフローインジェクション分析，*分析化学*, **2004**, 53, 291-296
5. Shinsuke Ohno, Norio Teshima, Tadao Sakai, Kate Grudpan, Miroslav Polasek
   Sequential Injection lab-on-valve simultaneous spectrophotometric determination of trace amounts of copper and iron, *Talanta*, **2006**, 68, 527-534